This is an open access article published under an ACS AuthorChoice License, which permits copying and redistribution of the article or any adaptations for non-commercial purposes.

JOURNAL OF NATURAL PRODUCTS

Article

Cite This: J. Nat. Prod. 2019, 82, 3150−3164

pubs.acs.org/jnp

Ealamines A−H, a Series of Naphthylisoquinolines with the Rare 7,8′-Coupling Site, from the Congolese Liana *Ancistrocladus ealaensis*, Targeting Pancreatic Cancer Cells

Dieudonné Tshitenge Tshitenge,[†,‡,§] Torsten Bruhn,[†,⊥] Doris Feineis,[†] David Schmidt,[†] Virima Mudogo,[∥] Marcel Kaiser,[¶,○] Reto Brun,[¶,○] Frank Würthner,[†] Suresh Awale,[*,#] and Gerhard Bringmann[*,†]

[†]Institute of Organic Chemistry, University of Würzburg, Am Hubland, D-97074 Würzburg, Germany

[‡]Faculty of Pharmaceutical Sciences, University of Kinshasa, B.P. 212 Kinshasa XI, Democratic Republic of the Congo

[§]Medicinal Chemistry, Bayer AG, Pharmaceuticals, Aprather Weg 18a, D-42096 Wuppertal, Germany

[⊥]Federal Institute for Risk Assessment, Max-Dohrn-Straße 8-10, D-10589 Berlin, Germany

[∥]Faculté des Sciences, Université de Kinshasa, B.P. 202, Kinshasa XI, Democratic Republic of the Congo

[¶]Swiss Tropical and Public Health Institute, Socinstrasse 57, CH-4002 Basel, Switzerland

[○]University of Basel, Petersplatz 1, CH-4003 Basel, Switzerland

[#]Division of Natural Drug Discovery, Institute of Natural Medicine, University of Toyama, 2630 Sugitani, Toyama 930-0194, Japan

Supporting Information

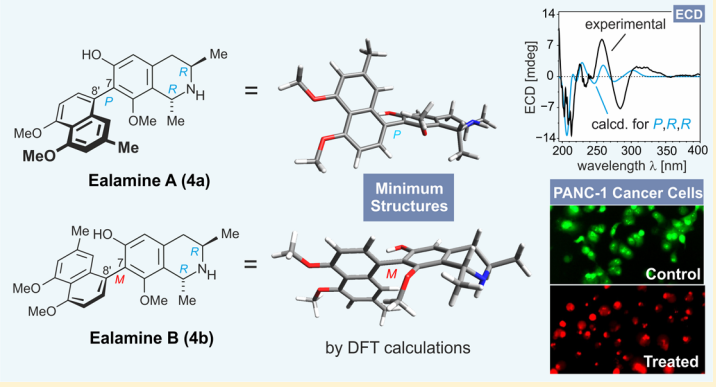

ABSTRACT: From the twigs and leaves of the Central African liana *Ancistrocladus ealaensis* (Ancistrocladaceae), a series of ten 7,8′-coupled naphthylisoquinoline alkaloids were isolated, comprising eight new compounds, named ealamines A−H (**4a**, **4b**, **5**−**10**), and two known ones, 6-*O*-demethylancistrobrevine A (**11**) and yaoundamine A (**12**), which had previously been found in related African *Ancistrocladus* species. Only one of the new compounds within this series, ealamine H (**10**), is a typical Ancistrocladaceae-type alkaloid, with 3*S*-configuration at C-3 and an oxygen function at C-6, whereas seven of the new alkaloids are the first 7,8′-linked "hybrid-type" naphthylisoquinoline alkaloids, i.e., 3*R*-configured and 6-oxygenated in the tetrahydroisoquinoline part. The discovery of such a broad series of 7,8′-coupled naphthyltetrahydroisoquinolines is unprecedented, because representatives of this subclass of alkaloids are normally found in Nature quite rarely. The stereostructures of the new ealamines were assigned by HRESIMS, 1D and 2D NMR, oxidative degradation, and experimental and quantum-chemical ECD investigations, and—in the case of ealamine A (**4a**)—also confirmed by X-ray diffraction analysis. Ealamines A−D exhibited distinct—and specific—antiplasmodial activities, and they displayed pronounced preferential cytotoxic effects toward PANC-1 human pancreatic cancer cells in nutrient-deprived medium, without causing toxicity under normal, nutrient-rich conditions, with ealamine C (**5**) as the most potent agent.

Naphthylisoquinoline alkaloids[1−3] are the only di- and tetrahydroisoquinoline natural products that are not, as usual, built up from aromatic amino acids,[4] but from acetate/malonate units, following a novel, polyketidic pathway to isoquinolines in plants.[5] Their two molecular halves, the naphthalene and the isoquinoline subunits, are formed separately, both from joint polyketide precursors, and are connected to each other at a quite late stage of the biosynthetic

Received: August 7, 2019
Published: October 20, 2019

ACS Publications © 2019 American Chemical Society and American Society of Pharmacognosy

DOI: 10.1021/acs.jnatprod.9b00755
J. Nat. Prod. 2019, 82, 3150−3164

Downloaded via UNIV OF BASEL on December 2, 2019 at 14:43:19 (UTC).
See https://pubs.acs.org/sharingguidelines for options on how to legitimately share published articles.

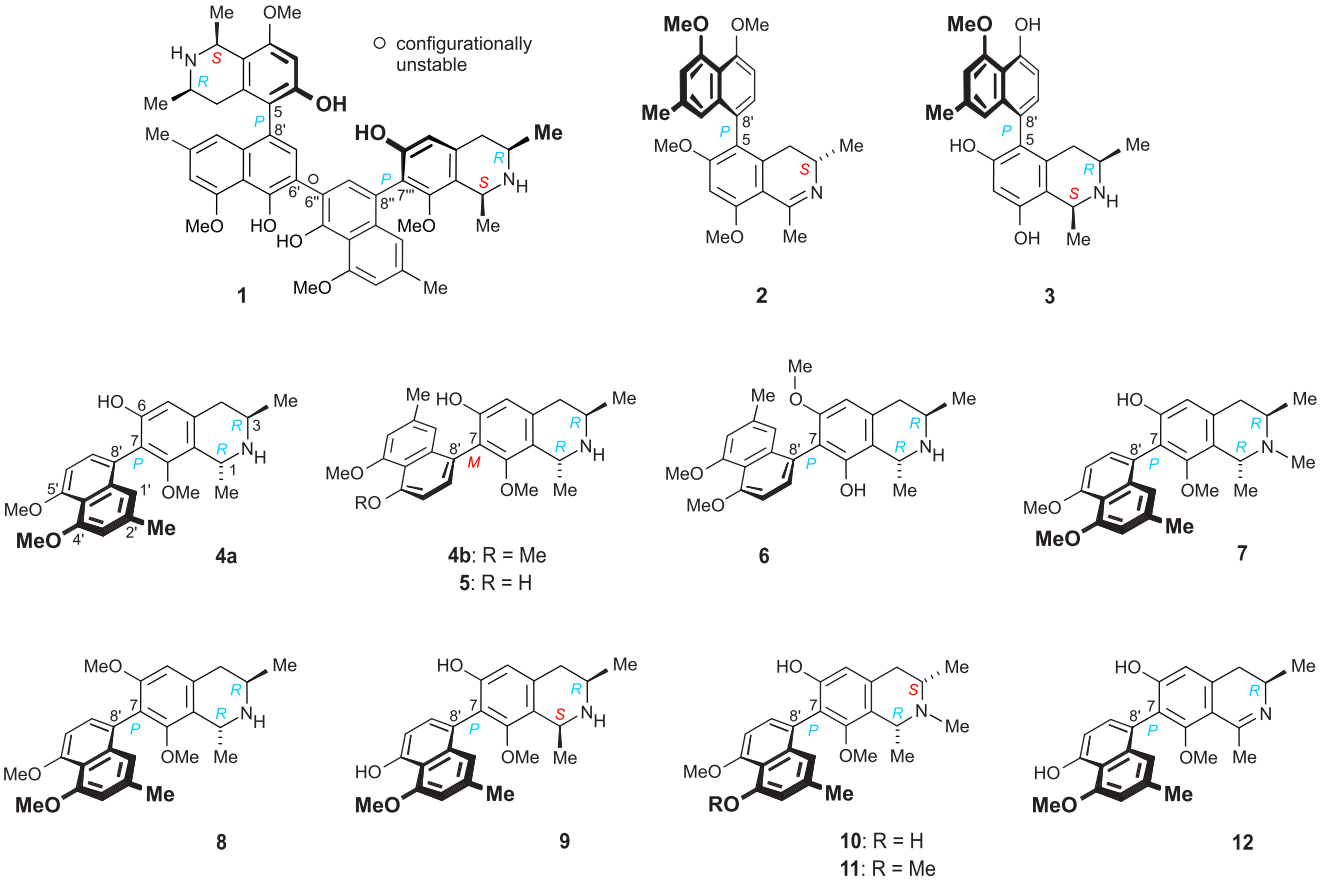

Figure 1. Naphthylisoquinoline alkaloids from the Central African liana *A. ealaensis*, among them a series of 10 compounds with the rare 7,8′-coupling type: the new ealamines A–H (**4a**, **4b**, **5**–**10**) and the known[31,32] alkaloids 6-*O*-demethylancistrobrevine A (**11**) and yaoundamine A (**12**), the latter two now detected for the first time in *A. ealaensis*; likewise shown are the previously identified dimer ealapasamine C (**1**),[10] a cross-coupling product of a 5,8′- and a 7,8′-linked naphthylisoquinoline, and the two 5,8′-coupled monomeric alkaloids ancistroealaines A (**2**)[9] and C (**3**).[11]

route,[1,5,6] by phenol-oxidative cross-coupling, which occurs *ortho* or *para* relative to free phenolic oxygen functions. Based on this principle, eight C,C-coupling types are imaginable, of which seven (viz., 5,1′, 5,3′, 5,8′, 7,1′, 7,3′, 7,6′, and 7,8′) have so far been discovered in Nature.[1−3]

The Congolese liana *Ancistrocladus ealaensis* J. Léonard[7,8] is a rich source of structurally diverse naphthylisoquinoline alkaloids.[9−12] Its metabolic profile differs completely from those of the three other known taxa likewise endemic to the Congo Basin, *A. congolensis*,[13,14] *A. likoko*,[15−18] and *A. ileboensis*,[19,20] but also from the profiles of further, botanically yet undescribed *Ancistrocladus* lianas[21−27] recently discovered in the rainforests of the Democratic Republic of the Congo. From *A. ealaensis*, a series of unusual heterodimers,[10−12] belonging to four subgroups of dimers, have been isolated, representing an unprecedented plethora of all these alkaloid types in the same plant. Among these compounds were four highly unsymmetric 6′,1″-coupled mbandakamines[11] consisting of two 5,8′-coupled monomers with three consecutive stereogenic axes identified along with a nearly symmetric michellamine-type dimer,[10] likewise built up from two 5,8′-coupled monomers, but linked via a freely rotating central 6′,6″-axis. Unprecedented was the discovery of seven oxygen-bridged mbandakamine-type dimers, named cyclombandakamines,[12] featuring an unusual condensed cage-like polycyclic backbone. In addition, three unusual heterodimers such as ealapasamine C (**1**)[9] (Figure 1) have been found in the leaves of *A. ealaensis*, containing two different biaryl moieties, viz., a 5,8′-coupled naphthylisoquinoline and a 7,8′-linked portion, with a central 6′,6″-coupled binaphthalene core.

Most of the Central African *Ancistrocladus* species produce predominantly 5,8′-linked mono- and dimeric naphthylisoquinoline alkaloids.[13−18,23−29] More than 90 alkaloids of this subclass have so far been isolated, among them typical Ancistrocladaceae-type[1,3] compounds such as ancistroealaine A (**2**),[9,23,26] with the *S*-configuration at C-3 and an oxygen function at C-6. In addition, a noticeable number of "hybrid-type"[1,3] naphthylisoquinolines have been identified such as ancistroealaine C (**3**)[11,25] (Figure 1), i.e., likewise oxygenated at C-6, but with an *R*-configuration at C-3. In contrast to the numerous 5,8′-coupled naphthylisoquinoline alkaloids, their 7,8′-linked analogues are far less common in Nature; only 20 such compounds (15 monomers[19,30−32] and five dimers[10,33,34]) have been detected so far in *Ancistrocladus* plants.

We report herein the isolation and structural elucidation of an unusual series of eight new 7,8′-coupled naphthylisoquinoline alkaloids, named ealamines A–H (**4a**, **4b**, and **5**–**10**) (Figure 1), from the twigs and leaves of *A. ealaensis*. They were discovered together with two known,[3,23,31,32] likewise 7,8′-linked metabolites, 6-*O*-demethylancistrobrevine A (**11**) and yaoundamine A (**12**), which had earlier been identified in related African *Ancistrocladus* species. Seven of the new metabolites, ealamines A–G (**4a**, **4b**, and **5**–**9**), are the first naturally occurring 7,8′-coupled "hybrid-type" naphthyl-

DOI: 10.1021/acs.jnatprod.9b00755
J. Nat. Prod. 2019, 82, 3150−3164

tetrahydroisoquinoline alkaloids. Prior to this isolation work, only two 7,8′-linked hybrid-type alkaloids have been described, viz., yaoundamine A (**12**) with a dihydroisoquinoline subunit (here likewise detected in *A. ealaensis*) and its 6-*O*-rhamnoside analogue, yaoundamine B, from the Cameroonian liana *A. korupensis*.[32]

The elucidation of the axial configuration of the new hybrid-type 7,8′-coupled naphthyltetrahydroisoquinolines with *R*-configuration at C-3 by 2D NMR measurements proved to be unexpectedly challenging, since the energetically preferred conformers of the tetrahydropyrido parts of the *M*-configured alkaloids ealamines B (**4b**) and C (**5**) were found to adopt an arrangement with both the nitrogen atom and C-3 being "down", and not, as in other investigated cases,[6,19] a half-chair conformation, i.e., with the nitrogen atom "up" and C-3 "down". This led to unexpected cross-peaks in the NOESY spectra, which seemed to be contradictory to the ones anticipated for **4b** and **5** regarding the initially assumed half-chair confirmation of their tetrahydroisoquinoline portions. Here we describe the application of quite time-demanding, yet selective NOESY experiments with mixing-time optimization, which finally permitted reliable configurational assignments of such 7,8′-linked hybrid-type alkaloids with an *M*-configuration at the axis, by diagnostically decisive long-range couplings across the biaryl axis. The assignment of the absolute axial configurations of the ealamines A–H (**1a**, **1b**, and **5**–**10**), as obtained by 2D NMR measurements, was confirmed by density functional theory (DFT) calculations of their minimum structures and by comparison of the experimental electronic circular dichroism (ECD) data with the calculated ones.

Furthermore, as part of our ongoing studies on the anti-infective potential of naphthylisoquinoline alkaloids,[1,9−13,19−27,30,31] the ealamines A–D (**4a**, **4b**, **5**, and **6**) were tested for their activities against protozoan parasites causing severe tropical diseases such as malaria tropica, Chagas' disease, African sleeping sickness, and leishmaniasis. In addition, they were investigated for their cytotoxic effects against PANC-1 human pancreatic cancer cells under nutrient-deprived conditions.

RESULTS AND DISCUSSION

Isolation and Structural Elucidation of Naphthylisoquinoline Alkaloids. Leaves and twigs of *A. ealaensis* were collected in the Eala Botanical Garden (Jardin Botanique d'Eala) near the town of Mbandaka in the northwestern part of the Democratic Republic of the Congo. The air-dried material was ground and exhaustively extracted with MeOH. After evaporation of the solvent, the crude extracts were macerated with water and then further processed by liquid–liquid partition using *n*-hexane and CH_2Cl_2. Fractionation of the CH_2Cl_2 layers by column chromatography (CC) and solid-phase extraction (SPE) using C_{18} reversed-phase silica gel provided several alkaloid-containing subfractions, which were subjected to preparative HPLC, permitting isolation of 10 pure compounds (Figure 1).

One of the metabolites identified in the twig extract was the known 7,8′-coupled alkaloid 6-*O*-demethylancistrobrevine A (**11**), which had earlier been detected in the West African liana *A. abbreviatus*[3,31] and in a botanically undescribed Congolese *Ancistrocladus* species.[23] With its *S*-configuration at C-3 and an oxygen function at C-6, this naphthyltetrahydroisoquinoline belongs to the subclass of Ancistrocladaceae-type naphthylisoquinolines. Besides **11**, the likewise 7,8′-linked, but hybrid-type naphthyldihydroisoquinoline yaoundamine A (**12**), previously only known to occur in *A. korupensis*,[32] was isolated from the twigs and leaves of *A. ealaensis*. All of the eight other naphthylisoquinoline alkaloids discovered in the MeOH/CH_2Cl_2 extracts of *A. ealaensis* are new.

Ealamine A (4a). According to the HRESIMS, the molecular formula of the first new metabolite, obtained as a brownish powder from an alkaloid-enriched subfraction of the leaf extract, was determined as $C_{25}H_{30}NO_4$ (*m*/*z* 408.21570, $[M + H]^+$). The ^{13}C NMR and DEPT-135 spectra indicated the presence of 25 nonequivalent carbon atoms, among them 16 aromatic ones. Comprehensive analysis of the ^1H and ^{13}C NMR data (Table 1) revealed the presence of a substituted

Table 1. ^1H (600 MHz) and ^{13}C (150 MHz) NMR Data of Ealamines A (4a) and B (4b) in Methanol-d_4 (δ in ppm)

	ealamine A (**4a**)		ealamine B (**4b**)	
no.	δ_H (*J* in Hz)	δ_C, type	δ_H (*J* in Hz)	δ_C, type
1	4.72, q (6.8)	50.1, CH	4.73, q (6.8)	50.0, CH
3	3.87, m	45.3, CH	3.88, m	45.3, CH
4_{eq}	3.15, dd (17.5, 4.8)	34.6, CH_2	3.20, dd (17.9, 4.9)	34.6, CH_2
4_{ax}	2.88, dd (17.5, 11.9)		2.88, dd (17.9, 11.7)	
5	6.56, s	111.3, CH	6.56, s	111.3, CH
6		157.7, C		157.8, C
7		121.7, C		121.7, C
8		157.6, C		157.6, C
9		118.7, C		118.6, C
10		133.0, C		133.0, C
1′	6.85, d (1.1)	119.2, CH	6.84, d (1.1)	119.2, CH
2′		137.7, C		137.7, C
3′	6.78, d (1.4)	109.9, CH	6.78, d (1.2)	109.9, CH
4′		158.7, C		158.7, C
5′		158.7, C		158.7, C
6′	6.94, d (8.1)	106.7, CH	6.95, d (8.1)	106.7, CH
7′	7.21, d (8.0)	130.9, CH	7.21, d (8.1)	131.0, CH
8′		124.6, C		124.5, C
9′		137.7, C		137.7, C
10′		117.5, C		117.5, C
CH_3-1	1.65, d (6.8)	19.6, CH_3	1.65, d (6.8)	19.6, CH_3
CH_3-3	1.51, d (6.3)	19.4, CH_3	1.51, d (6.3)	19.5, CH_3
OCH_3-8	3.07, s	60.8, CH_3	3.07, s	60.8, CH_3
CH_3-2′	2.31, s	22.2, CH_3	2.31, s	22.2, CH_3
OCH_3-4′	3.93, s	57.1, CH_3	3.93, s	57.1, CH_3
OCH_3-5′	3.96, s	56.9, CH_3	3.96, s	56.9, CH_3

naphthalene spin system with four aromatic methines, H-1′ (δ_H 6.85), H-3′ (δ_H 6.78), H-6′ (δ_H 6.94), and H-7′ (δ_H 7.21), two methoxy functions, MeO-4′ ($\delta_{H,C}$ 3.93, 57.1) and MeO-5′ ($\delta_{H,C}$ 3.96, 56.9), and one aromatic methyl group, Me-2′ ($\delta_{H,C}$ 2.31, 22.2). An additional spin system corresponding to a tetrahydroisoquinoline subunit was assigned according to a shielded aromatic proton at δ_H 6.56 (H-5), two unshielded aliphatic methines at δ_H 4.72 (H-1) and 3.87 (H-3), two diastereotopic protons, H_{eq}-4 (δ_H 3.15) and H_{ax}-4 (δ_H 2.88), one shielded aromatic methoxy group, MeO-8 ($\delta_{H,C}$ 3.07, 60.8), and two methyl groups, Me-1 ($\delta_{H,C}$ 1.65, 19.6) and Me-3 ($\delta_{H,C}$ 1.51, 19.4) (Figure 2A). The normal, not high-field-shifted signal of Me-2′ (δ_H 2.31) excluded the biaryl axis from being located at C-1′ or C-3′, thus leaving only C-8′ and C-6′

DOI: 10.1021/acs.jnatprod.9b00755
J. Nat. Prod. 2019, 82, 3150−3164

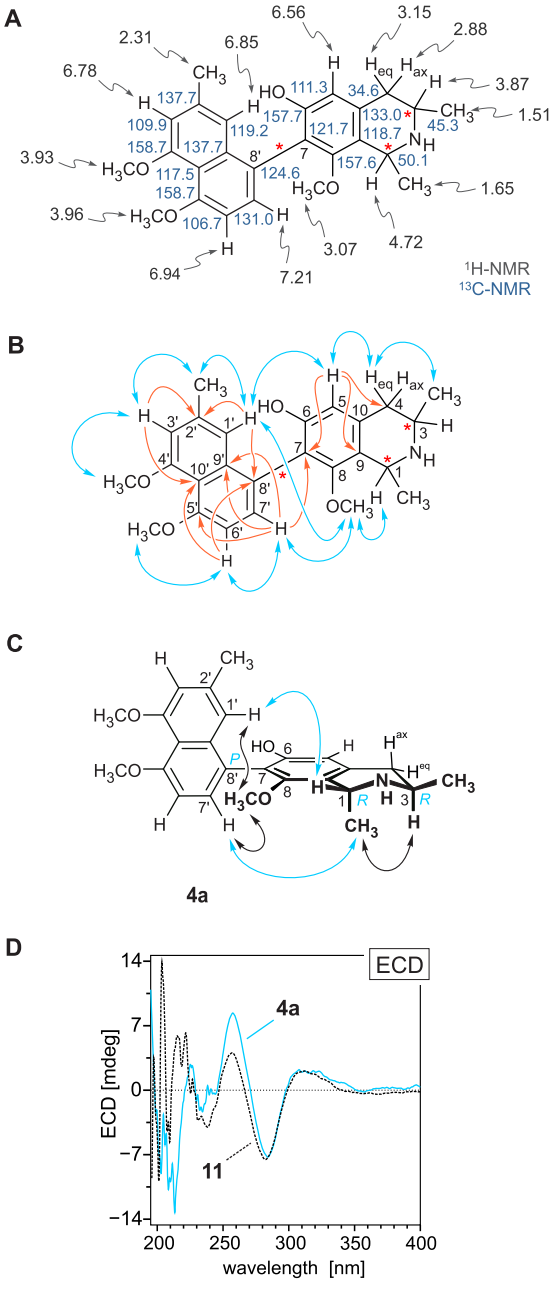

Figure 2. (A) Selected ^{1}H and ^{13}C NMR shifts (in methanol-d_4, δ in ppm) of ealamine A (**4a**), (B) key NOESY (double blue arrows) and HMBC (single orange arrows) interactions indicative of the constitution of **4a**, (C) decisive NOESY correlations (double blue arrows) defining the relative configuration of **4a** at the stereogenic centers versus the biaryl axis, and (D) absolute axial configuration of **4a** assigned by comparison of its ECD spectrum with that of the known[23,31] related 7,8′-coupled alkaloid 6-*O*-demethylancistrobrevine A (**11**).

as the coupling positions. The NOESY correlation sequence in the series {MeO-5′ ↔ H-6′ ↔ H-7′} showed that C-6′ could not be the axis-bearing carbon atom, thus revealing that the naphthalene portion is coupled via C-8′. This assignment was proven by HMBC interactions from H-1′ to the quaternary carbon atom C-8′ (δ_C 124.6) and from H-7′ to C-9′ (δ_C 137.7) and C-5′ (δ_C 158.7). The attribution of H-1′ and H-3′, in turn, was deduced from the NOESY correlation sequence {H-1′ ↔ Me-2′ ↔ H-3′ ↔ MeO-4′} and from HMBC interactions, each, from H-1′ and H-3′ to C-2′ (Figure 2B). A NOESY correlation between H-5 and H_{eq}-4 and HMBC interactions of H-5 to C-4 suggested the presence of a tetrahydroisoquinoline portion with no substituent at C-5, thus leaving the coupling position to be located at C-7. This result was confirmed by a series of further C−H correlations involving C-7 and C-8′: C-7 exhibited a ^{3}J interaction with H-5 in the tetrahydroisoquinoline subunit and a ^{4}J correlation with H-7 across the biaryl axis, while, vice versa, C-8′ displayed ^{3}J couplings to H-6′ and H-10′ and a ^{4}J HMBC interaction with H-5 (Figure 2B).

From a NOESY correlation between Me-1 (δ_H 1.65) and H-3 (δ_H 3.87), the relative configuration at C-1 versus C-3 in the tetrahydroisoquinoline part (Figure 2C) was deduced to be *trans*. The absolute configurations at C-1 and C-3 were determined by ruthenium-mediated oxidative degradation as described earlier,[35] with ensuing stereochemical analysis of the resulting amino acids by gas chromatography with mass-selective detection (GC-MSD) after derivatization with the *R*-enantiomer of Mosher's acid chloride. The formation of *R*-3-aminobutyric acid and D-alanine established the new alkaloid to be *R*-configured at both C-1 and C-3. The configuration at the biaryl axis relative to the stereogenic centers was deduced from a long-range NOESY interaction between H-7′ and Me-1, indicating that these two spin systems are on the same side of the isoquinoline plane, which, in conjunction with the *R*-configuration at C-3, should be the upper side, so that the biaryl axis should be *P*-configured, as illustrated in Figure 2C. This stereochemical attribution was confirmed by the complementary NOESY correlation between H-1′ and H-1, which were, thus, both on the bottom side of the molecule. The axial *P*-configuration was corroborated by the ECD spectrum of the new metabolite displaying a negative Cotton effect at 213 nm ($\Delta\varepsilon$, −13.3) and a positive one at 257 nm ($\Delta\varepsilon$, +8.4), which was in accordance with the ECD curve of the known, likewise 7,8′-coupled and *P*-configured—and co-occurring—alkaloid 6-*O*-demethylancistrobrevine A (**11**)[23,31] (Figure 2D). The new naphthylisoquinoline was thus found to be 1*R*,3*R*,7*P*-configured and, consequently, possesses the full absolute stereostructure **4a** as outlined in Figure 1. Owing to its isolation from *A. ealaensis*, it was given the name ealamine A.

The constitution and the relative configuration of ealamine A (**4a**) were additionally confirmed by single-crystal X-ray diffraction analysis (Figure 3). Naphthylisoquinoline alkaloids are usually difficult to crystallize without prior chemical derivatization,[28,36] and only very few X-ray structure analyses have so far succeeded.[21,28,36,37] In the case of **4a**, crystals of suitable quality were obtained by slow diffusion of *n*-hexane into a solution of **4a** in acetone at room temperature in the presence of trifluoroacetic acid. The crystal structure of ealamine A (**4a**) in its *N*-protonated form (trifluoroacetate, TFA salt), together with one molecule of acetone, as illustrated in Figure 3, fully confirmed the anticipated constitution and relative configuration of this new alkaloid as established above. Furthermore, based on the results of the oxidative degradation, the X-ray diffraction analysis firmly corroborated **4a** to be 1*R*,3*R*,7*P*-configured. It also showed the expected half-chair conformation in the heterocyclic tetrahydropyrido ring, with H-3 and the methyl group at C-1 in axial positions, while Me-3 and H-1 were equatorial.

Ealamine B (4b). HRESIMS analysis of the second compound isolated from the same leaf subfraction containing

DOI: 10.1021/acs.jnatprod.9b00755
J. Nat. Prod. 2019, 82, 3150−3164

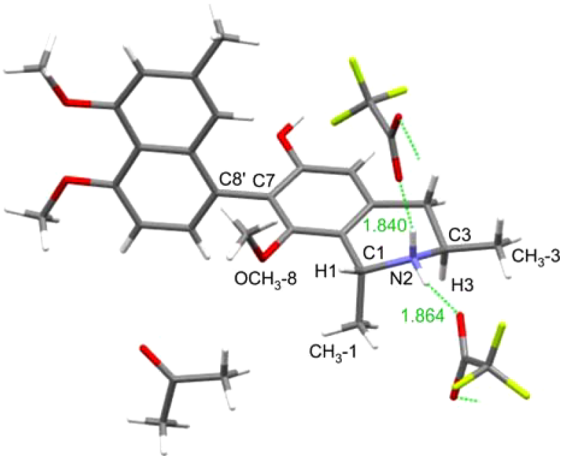

Figure 3. ORTEP drawing of the crystal structure of ealamine A (**4a**) as its trifluoroacetate (TFA) salt crystallized together with one molecule of acetone per two molecules of **4a**·TFA (carbon: gray; nitrogen: blue; oxygen: red). The equatorial hydrogen, H_{eq}, at the nitrogen atom is linked via a hydrogen bond to the oxygen of a trifluoroacetate anion, and the axial one, H_{ax}, is likewise connected to yet another trifluoroacetate anion, thus forming a chain $F_3C-CO-O^-\cdots H_{eq}-N^+R_2-H_{ax}\cdots{}^-O-OC-CF_3$ in the crystal lattice, continued by hydrogen bonding of the second oxygen function in the TFA molecules to further ealamine molecules.

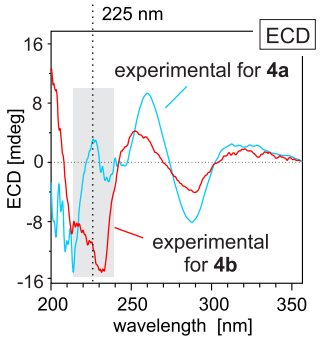

Figure 4. Comparison of the experimental ECD spectrum (monitored in methanol) of ealamine B (**4b**) with that of eleamine A (**4a**). The diagnostically decisive bandwidth around 225 nm is marked in gray.

ealamine A (**4a**), yet occurring in distinctly lower quantities and eluting more rapidly on the RP18 material, gave a molecular formula of $C_{25}H_{29}NO_4$, i.e., the same as **4a**. The new metabolite exhibited proton signals with coupling patterns and coupling constants in the ^{1}H NMR spectrum (Table 1) almost identical to those of **4a**, thus suggesting that the compound is a stereoisomer of **4a**. Like for compound **4a**, it was again a 7,8′-coupled naphthyltetrahydroisoquinoline, as deduced from HMBC interactions from H-7′ (δ_H 7.21) to C-7 (δ_C 121.7) and from H-1′ (δ_H 6.84) to C-8′ (δ_C 124.5). This was evidenced further by the upfield-shifted signal of MeO-8 (δ_H 3.07), from an NOE cross-peak from H-4$_{eq}$ (δ_H 3.20) to a singlet at δ_H 6.56, which had to be H-5, and from NOESY correlations between MeO-8 and H-1′ and between MeO-8 and H-7′. Moreover, similar to **4a**, the new compound possesses two *O*-methyl groups (δ_H 3.93 and 3.96) at C-4′ and C-5′ in the naphthalene subunit, as deduced from NOESY interactions to H-3′ (δ_H 6.78) and H-6′ (δ_H 6.95), respectively. The fourth oxygen function thus had to be a free phenolic hydroxy group at C-6 in the isoquinoline part. Hence, the isolated metabolite had the same constitution as **4a**, yet being configurationally different.

A NOESY cross-peak of the protons of Me-1 (δ_H 1.65) to H-3 (δ_H 3.88) was used to assign the methyl groups at C-1 and C-3 as *trans* to one another (Figure 5, bottom). The oxidative degradation[35] procedure again delivered only D-alanine and *R*-3-aminobutyric acid, and, thus, together with the relative *trans*-configuration, the absolute configurations of the two stereogenic centers in the tetrahydroisoquinoline subunit were—as in the case of **4a**—attributed as 1*R*,3*R*. Hence, ealamine A (**4a**) and the new naphthylisoquinoline alkaloid were most likely a pair of atropo-diastereomers. Accordingly, the second new metabolite should be *M*-configured at the biaryl axis.

Comparison of the ECD spectrum of the new alkaloid with that of ealamine A (**4a**) revealed these two compounds to display an opposite curve around 225 nm (see gray zone and dotted line in Figure 4). Remarkably, the negative Cotton effect at 230 nm ($\Delta\varepsilon$, −15.8) monitored for the new alkaloid was quite strong compared to the weak positive one at 225 nm ($\Delta\varepsilon$, +3.8) observed for **4a**. This opposite ECD behavior of the two alkaloids in the decisive part of the spectrum for the biaryl chromophore supported the assumption that the second metabolite isolated from the leaf extract of *A. ealaensis* should be *M*-configured, thus possessing the structure **4b** (see Figure 1). For other wavelengths, the ECD curves of **4a** and **4b**, however, showed different, not fully reversed shapes. In many cases,[1−3,21,27,31] the ECD spectra of atropo-diastereomers are virtually opposite of each other, because the chiroptical behavior is largely dominated by the stronger biaryl chromophore and, thus, by the axial configuration. On the other hand, since the two apparently atropisomeric naphthylisoquinoline alkaloids—**4a** and **4b**—were diastereomers and not enantiomers, the appearance of nonopposite, but divergent ECD spectra should not be totally excluded.[38] Apparently, the chromophore-related parts of the molecules were not fully mirror-image-like in this case, probably as a consequence of conformational divergences concerning the dihedral angles at the axes of these two alkaloids due to the different relative configurations in these two atropo-diastereomeric alkaloids.

The assignment of the absolute axial configuration of the new compound **4b** to be *M* was in agreement with a long-range NOESY correlation between Me-2′ (δ_H 2.31) and Me-1 (δ_H 1.65) (Figure 5, bottom). On the other hand, the likewise expected cross-peak between H-1′ (δ_H 6.84) and Me-1 was not found in the NOESY spectrum of **4b**, but another—seemingly contradictory—long-range NOESY interaction between Me-1 and H-7′ (δ_H 7.21) was observed, the latter two spectroscopic values apparently consistent with a *P*-configuration, as in ealamine A (**4a**). Such—at first sight conflicting—interactions had never been observed in any other naphthylisoquinoline alkaloid before. A rational explanation resulted from a comparative conformational analysis of **4a** and **4b** by DFT calculations using the B3LYP-3D/def2-SVP method. These investigations revealed that **4a** occurred mainly in a half-chair conformation **4a-I**, i.e., with the nitrogen atom "up" and C-3 "down" (see Figure 5, top, center). The most populated conformer of **4b**, by contrast, was not the corresponding half-chair form **4b-I** (see Figure 5, bottom, left), but the tetrahydroisoquinoline portion of the new compound **4b** was found to preferably adopt the conformation **4b-II** (see Figure 5, bottom, center), with both the nitrogen and C-3 "down" and with Me-1 now occupying a pseudoequatorial position and, in

DOI: 10.1021/acs.jnatprod.9b00755
J. Nat. Prod. 2019, 82, 3150−3164

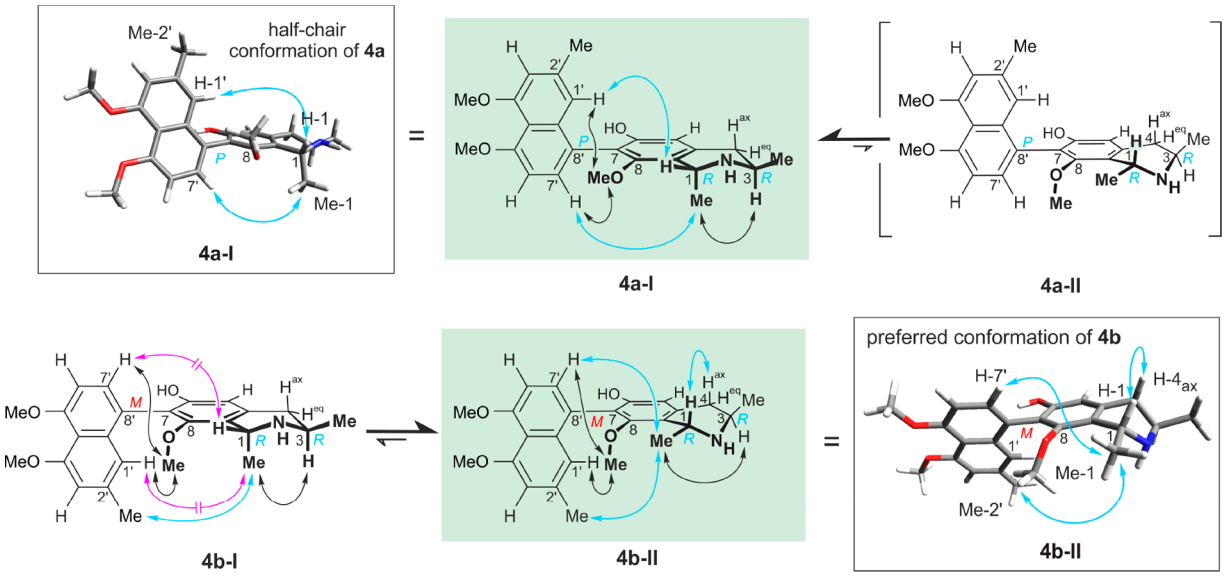

Figure 5. Divergent conformational equilibria in the partially saturated heterocyclic rings of ealamine A (**4a**) and ealamine B (**4b**), as evident from DFT calculations of the molecular minimum structures of **4a** and **4b** and decisive NOESY interactions (double blue arrows) defining the relative configuration at the stereogenic centers versus the biaryl axis of **4a** and **4b**. The single-point energy difference between the low-populated species **4b-I** and the most stable one, **4b-II**, was calculated as ΔE = 3 kcal/mol, leading to a slightly shifted population between these different conformers in favor of conformation type **I** for **4a** and conformation type **II** for **4b**.

turn, with H-1 becoming pseudoaxial. Such a rarely observed array has been referred to as a half-boat conformation in the literature.[39] With the Me-1 group in **4b-II** in an equatorial position, the spatial distance to H-1′ was largely increased (up to ca. 4.7 Å), now, instead, permitting detection of an unexpected long-range NOE interaction between Me-1 and H-7′, which would not have been imaginable in the case of **4b-I**. For **4b-II**, the steric position of H-1 was also in agreement with the NOE correlation of H-1 (δ_H 4.73) to H_{ax}-4 (δ_H 2.88), both now occupying an axial position, with a relatively short computed distance of 2.331 Å. These unexpected conformational peculiarities had never been observed before within this class of alkaloids.

The calculations also showed that in the case of ealamine B (**4b**), and different from that of ealamine A (**4a**), H-1′ was largely shielded by the methoxy group at C-8 and was, thus, prevented from NOE interactions with Me-1. In consequence, the two atropo-diastereomers **4a** and **4b** were clearly distinguishable by the long-range NOESY interaction between Me-1 and Me-2′, as found only in **4b**, not in **4a** (and not in any other comparable naphthyltetrahydroisoquinoline). This correlation had thus become the decisive one for an unambiguous attribution of an *M*-configuration at the biaryl axis of the 7,8′-coupled naphthylisoquinoline alkaloid presented in this paper.

Accordingly, also in view of the fact that the new metabolite **4b** had the same constitution as **4a** and the same relative and absolute configurations at the two stereocenters C-1 and C-3 in the tetrahydroisoquinoline subunit, this alkaloid was indeed the atropo-diastereomer of **4a** and, thus, had to be *M*-configured at the biaryl axis, hence possessing the full absolute stereostructure **4b** as shown in Figure 1. It was named ealamine B.

For a further confirmation of the absolute configurations at the biaryl axis of the ealamines A (**4a**) and B (**4b**), quantum-chemical ECD calculations at the TD-CAM-B3LYP/def2-TZVP(-f) level were performed. The ECD spectrum theoretically predicted for the *P,R,R*-atropo-diastereomer was in good agreement with the respective curve measured for ealamine A (**4a**), and the spectrum calculated for the *M,R,R*-atropo-diastereomer was in accordance with the experimental ECD curve of ealamine B (**4b**) (Figure 6).

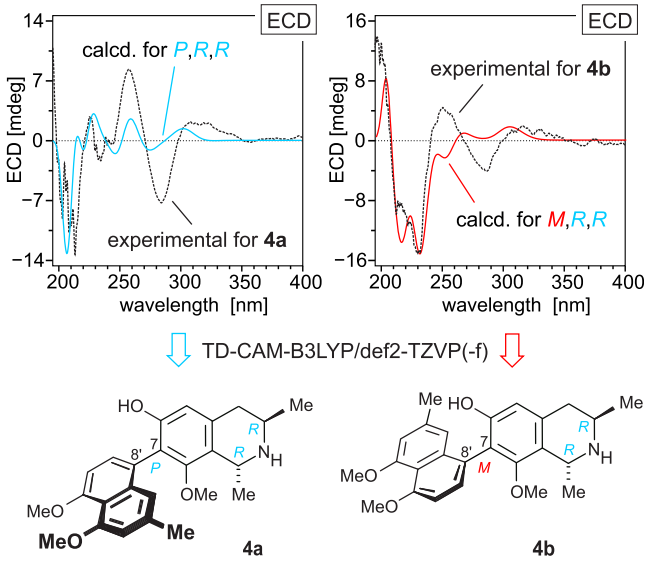

Figure 6. Assignment of the absolute configurations of ealamine A (**4a**) and its atropo-diastereomer ealamine B (**4b**) by comparison of the experimental ECD curves (monitored in methanol) with the spectra calculated for the *P*- and the *M*-atropo-diastereomers using TD-CAM-B3LYP/def2-TZVP(-f).

Ealamine C (5). The third metabolite isolated from the leaves of *A. ealaensis* was obtained as an optically active brownish powder. According to the HRESIMS, this corresponded to a molecular formula of $C_{24}H_{27}NO_4$. The most significant difference between the NMR data of the new compound (Tables 2 and 3) when compared to those of **4a** and **4b** was a missing *O*-methyl group. NOESY interactions

DOI: 10.1021/acs.jnatprod.9b00755
J. Nat. Prod. 2019, 82, 3150−3164

Table 2. ^{1}H (600 MHz) NMR Data of Ealamines C−H (5−10) in Methanol-d_4 (δ in ppm)

	ealamine C (5)	ealamine D (6)	ealamine E (7)	ealamine F (8)	ealamine G (9)	ealamine H (10)
no.	δ_H (J in Hz)	δ_H (J in Hz)	δ_H (J in Hz)	δ_H (J in Hz)	δ_H (J in Hz)	δ_H (J in Hz)
1	4.72, q (6.7)	4.90, q (6.9)	4.66, q (6.8)	4.77, q (6.9)	4.68, q (6.5)	4.60, q (6.9)
3	3.86, m	3.89, m	4.15, m	3.90, m	3.49, m	3.47, m
4_{eq}	3.14, dd (17.8, 4.8)	3.16, dd (17.4, 5.6)	3.12, dd (18.8, 5.0)	3.22, dd (16.7, 4.5)	2.96, pd (7.5)	3.01, pd (7.05)
4_{ax}	2.88, dd (17.6, 11.7)	2.86, dd (18.3, 11.7)	2.96, dd (18.8, 12.0)	2.96, dd (18.1, 11.7)	2.96, pd (7.5)	3.01, pd (7.05)
5	6.56, s	6.57, s	6.58, s	6.74, s	6.58, s	6.60, s
1′	6.85, br s	6.80, br s	6.89, s	6.79, br s	6.85, br s	6.74, s
3′	6.79, d (1.2)	6.79, s	6.79, s	6.76, d (1.2)	6.80, d (1.1)	6.66, d (1.3)
6′	6.80, d (7.9)	6.94, d (8.0)	6.94, d (8.3)	6.94, d (8.1)	6.80, d (7.9)	6.95, d (8.1)
7′	7.16, d (7.9)	7.22, d (8.0)	7.19, d (8.0)	7.18, d (7.9)	7.17, d (7.9)	7.19, d (8.0)
CH_3-1	1.64, d (6.8)	1.65, d (6.8)	1.65, d (6.8)	1.68, d (6.9)	1.72, d (6.6)	1.75, d (6.7)
CH_3-3	1.51, d (6.4)	1.51, d (6.5)	1.51, d (6.3)	1.55, d (6.5)	1.51, d (6.5)	1.60, d (6.5)
N-CH_3			2.87, s			3.08, s
OCH_3-6		3.15, s		3.64, s		
OCH_3-8	3.07, s		3.07, s	3.11, s	3.13, s	3.09, s
CH_3-2′	2.32, br s	2.31, s	2.31, s	2.31, br s	2.34, br s	2.27, br s
OCH_3-4′	4.08, s	3.96, s	3.93, s	3.95, s	4.09, s	
OCH_3-5′		3.93, s	3.96, s	3.98, s		4.12, s

Table 3. ^{13}C (150 MHz) NMR Data of Ealamines C−H (5−10) in Methanol-d_4 (δ in ppm)

	ealamine C (5)	ealamine D (6)	ealamine E (7)	ealamine F (8)	ealamine G (9)	ealamine H (10)
no.	δ_C, type	δ_C, type	δ_C, type	δ_C, type	δ_C, type	δ_C, type
1	50.0, CH	49.8, CH	60.5, CH	50.0, CH	52.5, CH	62.8, CH
3	45.3, CH	45.3, CH	50.6, CH	45.3, CH	51.3, CH	60.9, CH
4	34.6, CH_2	34.6, CH_2	30.4, CH_2	34.6, CH_2	35.3, CH_2	35.3, CH_2
5	111.3, CH	111.5, CH	111.1, CH	111.3, CH	111.9, CH	111.2, CH
6	157.8, C	157.7, C	157.8, C	157.8, C	157.6, C	157.7, C
7	121.7, C	121.5, C	121.9, C	121.7, C	122.0, C	121.9, C
8	157.6, C	157.8, C	158.2, C	157.6, C	158.7, C	157.7, C
9	118.6, C	118.5, C	117.3, C	118.6, C	118.9, C	118.5, C
10	133.0, C	133.0, C	130.8, C	133.0, C	134.8, C	134.7, C
1′	119.9, CH	119.4, CH	119.1, CH	119.9, CH	120,0, CH	117.6, CH
2′	137.4, C	137.7, C	137.6, C	137.4, C	137.3, C	139.0, C
3′	107.5, CH	109.9, CH	109.8, CH	107.5, CH	107.5, CH	113.1, CH
4′	157.9, C	158.7, C	158.6, C	157.9, C	157.9, C	156.3, C
5′	156.1, C	158.6, C	158.6, C	156.1, C	156.1, C	157.9, C
6′	110.4, CH	106.5, CH	106.5, CH	110.4, CH	110.2, CH	104.5, CH
7′	131.9, CH	130.9, CH	130.8, CH	131.9, CH	131.7, CH	130.4, CH
8′	122.6, C	124.6, C	124.4, C	122.6, C	122.8, C	125.7, C
9′	137.0, C	137.6, C	137.6, C	137.0, C	137.1, C	137.2, C
10′	114.8, C	117.6, C	116.3, C	114.8, C	114.9, C	114.8, C
CH_3-1	19.6, CH_3	19.6, CH_3	20.2, CH_3	19.6, CH_3	20.7, CH_3	20.8, CH_3
CH_3-3	19.4, CH_3	19.4, CH_3	16.8, CH_3	19.4, CH_3	19.0, CH_3	18.3, CH_3
N-CH_3			34.2, CH_3			42.0, CH_3
OCH_3-6		61.1, CH_3		56.9, CH_3		
OCH_3-8	60.7, CH_3		60.7, CH_3	60.7, CH_3	60.8, CH_3	60.9, CH_3
CH_3-2′	22.4, CH_3	22.2, CH_3	22.1, CH_3	22.4, CH_3	22.4, CH_3	22.1, CH_3
OCH_3-4′	56.9, CH_3	56.9, CH_3	56.9, CH_3	56.9, CH_3	56.9, CH_3	
OCH_3-5′		57.1, CH_3	56.7, CH_3	56.9, CH_3		56.9, CH_3

from H-3′ (δ_H 6.79) to MeO-4′ (δ_H 4.08) and from MeO-8 (δ_H 3.07) to H-1′ (δ_H 6.85) and to H-7′ (δ_H 7.16) revealed the presence of a free phenolic hydroxy group, located at C-5′ (Figure 7A). Like in **4a** and **4b**, the relative configuration of the two methyl groups at C-1 versus C-3 was deduced to be *trans* from specific NOE interactions, and again the absolute configurations in the tetrahydroisoquinoline subunit were assigned as 1*R*,3*R* by ruthenium-mediated oxidative degradation.[35] ECD spectroscopy established the compound to be *M*-configured at the biaryl axis (Figure 7C). Similar to ealamine B (**4b**), an NOE cross-peak from Me-1 (δ_H 1.64) to Me-2′ (δ_H 2.32) was observed, along with interactions between Me-1 and H-7′ (δ_H 7.16) and between H-1 (δ_H 4.72) and H_{ax}-4 (δ_H 2.88) (Figure 7A), which were found to be indicative of an axial *M*-configuration. Calculations using the ORCA[40] software package gave rise to a preferential minimum structure of the new metabolite showing the same unusual three-dimensional arrangement in the tetrahydroisoquinoline subunit as found for

DOI: 10.1021/acs.jnatprod.9b00755
J. Nat. Prod. 2019, 82, 3150−3164

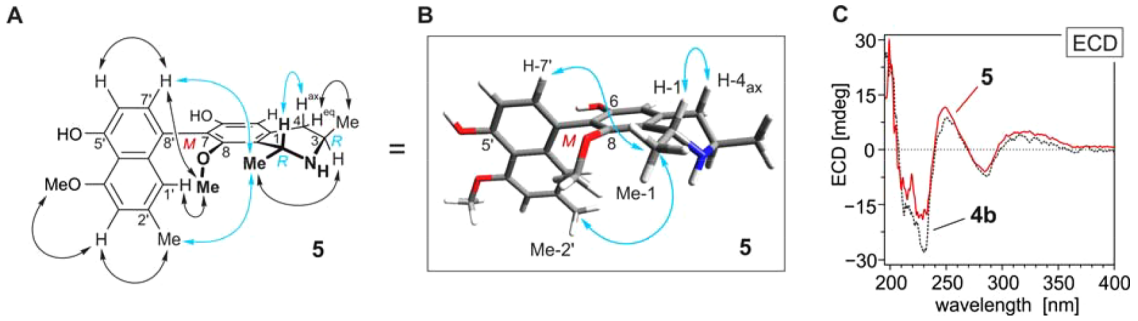

Figure 7. (A) Key NOESY (double black arrows) interactions indicative of the constitution of ealamine C (**5**) and decisive NOESY correlations defining its relative configuration at the stereogenic centers C-1 and C-3 in the tetrahydroisoquinoline subunit versus the biaryl axis (double blue arrows), (B) DFT-optimized structure of **5**, as obtained from calculations using the B3LYP-D3/def2-SVP method, and (C) confirmation of the absolute axial configuration of **5** by comparison of its experimental ECD spectrum with that of ealamine B (**4b**).

4b, i.e., type **II** (see **4b-II** in Figure 5), with both the nitrogen atom and C-3 adopting a "down" position (Figure 7C). Again, the half-chair conformation was not predominant. This corroborated that such a previously unrecognized conformational preference of the tetrahydroisoquinoline portion, with both the nitrogen atom and C-3 "down", was linked to the spatial orientation of the two chromophores within the series of so far quite rare *M*-configured 7,8′-coupled naphthylisoquinoline alkaloids.[6,19,30] The new alkaloid thus possessed the full stereostructure **5** (Figure 1) and was named ealamine C.

Ealamine D (6). Along with ealamine C (**5**), a fourth compound was isolated, albeit in very small quantities, with a molecular formula identical to those of **4a** and **4b**. ^{1}H (Table 2) and ^{13}C NMR (Table 3) data and specific NOE correlations (see Figure 8A) revealed the presence of yet another naphthyltetrahydroisoquinoline alkaloid belonging to the rare 7,8′-coupling type. When compared with **4a** and **4b**, it differed by its OH/OMe substitution pattern in the tetrahydroisoquinoline portion, possessing a methoxy group (δ_H 3.15) at C-6 and a free phenolic hydroxy function at C-8. As for **4a** and **4b**, a relative *trans*-configuration between the two stereocenters at C-1 and C-3 was evident from a NOESY interaction between H-3 (δ_H 3.89) and Me-1 (δ_H 1.65). The absolute configurations at the stereogenic centers, as determined by oxidative degradation,[35] were again *R*, both for C-1 and C-3. From its nearly identical ECD spectrum compared to that of **4b** (see Supporting Information), the isolated minor alkaloid had the same axial configuration, yet, merely for formal reasons, according to the Cahn–Ingold–Prelog rules, now denoted as *P*-configured. This stereochemical assignment was corroborated by the decisive long-range NOE interaction between Me-1 and Me-2′ (δ_H 2.31) like in **4b** and **5**. Now, however, due to the lacking 8-*O*-methyl group as in the case of the previous examples, ealamines B (**4b**) and C (**5**), also the characteristic cross-peak from Me-1 to H-1′ (δ_H 6.80) was observed for this new alkaloid (Figure 8A). Again, the DFT-optimized minimum structure of the isolated metabolite displayed a conformation of type **II** (see **4b-II** in Figure 5) for the most populated conformer, with H-1′, Me-1, and H-3 being located on the same side of the molecule (Figure 8B). The new alkaloid thus possessed the absolute stereostructure **6** (Figure 1). It was named ealamine D.

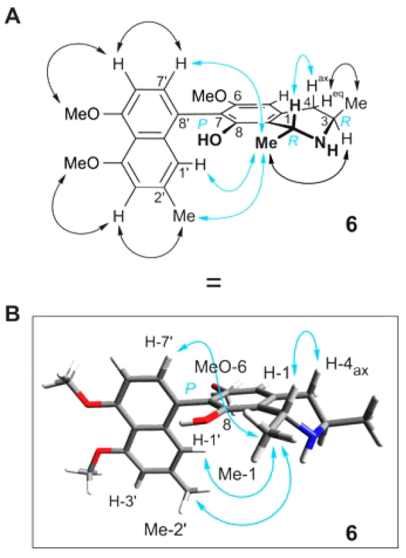

Figure 8. (A) Decisive NOESY (double blue arrows) cross-peaks proving the relative configuration of ealamine D (**6**) at the biaryl axis and at the stereogenic centers C-1 and C-3 in the tetrahydroisoquinoline part. (B) DFT-optimized structure of **6**, based on the B3LYP-D3/def2-SVP method.

Ealamines E (7) and F (8). The fifth and the sixth new alkaloids, also isolated from the leaves of *A. ealaensis*, showed ^{1}H and ^{13}C NMR data suggesting the presence of naphthyltetrahydroisoquinoline alkaloids again belonging to the 7,8′-coupling type. Their constitutions strongly resembled that of the above-presented ealamine A (**4a**), yet with a higher degree of methylation. According to the HRESIMS, both compounds corresponded to a molecular formula of $C_{26}H_{31}NO_4$. The ^{1}H NMR spectrum (Table 3) of the fifth compound—in contrast to that of **4a**—showed four methyl groups, resonating at δ_H 1.51, 1.65, 2.31, and 2.87. The latter signal was typical of an *N*-methyl group, while the NOESY correlation series {H_{eq}-4 ↔ H-5 ↔ OMe-6} clearly revealed the sixth compound to possess a methoxy function at C-6 (δ_H 3.64).

By the above-mentioned methods—the oxidative degradation, specific NOESY interactions across the biaryl axis, DFT calculations of the minimum structure, and ECD spectroscopy (see Supporting Information)—the two new alkaloids were established to be *R*-configured, at both C-1 and C-3, and *P*-configured at the axis, similar to ealamine A (**4a**). The fifth metabolite had the complete stereostructure **7** (Figure 1). It was found to be a new *N*-methyl analogue of **4a** and was named ealamine E. The sixth alkaloid, which is the 6-*O*-methyl

DOI: 10.1021/acs.jnatprod.9b00755
J. Nat. Prod. 2019, 82, 3150–3164

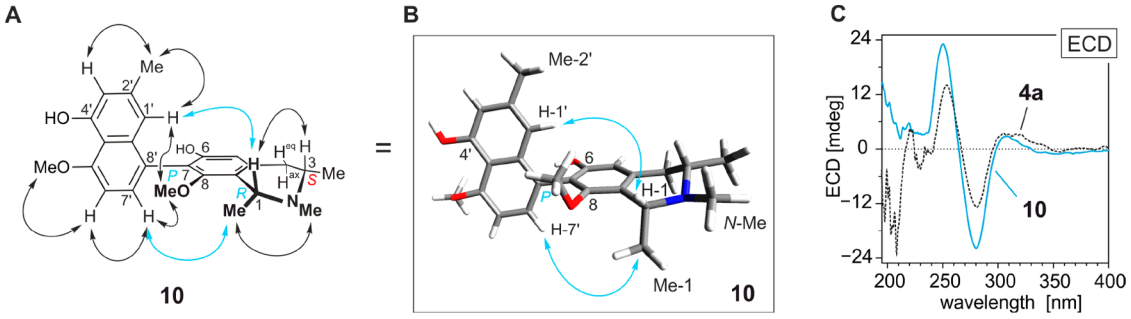

Figure 9. (A) Key NOESY interactions defining the relative configuration of ealamine H (**10**) at the stereogenic centers C-1 and C-3 in the tetrahydroisoquinoline portion and relative to the biaryl axis (decisive cross-peaks are marked in blue), (B) DFT-optimized structure of **10**, obtained from calculations using the B3LYP-D3/def2-SVP method, and (C) confirmation of the absolute axial configuration of **10** by comparison of its experimental ECD spectrum with that of ealamine A (**4a**).

Table 4. Antiprotozoal Activities of Ealamines A (4a), B (4b), C (5), and D (6) against Pathogens of the Genera *Plasmodium*, *Trypanosoma*, and *Leishmania* and Their Cytotoxicities against Rat Skeletal Myoblast (L6) Cells

	IC_{50} [μM][a]						
compound	*P. falciparum* (NF54)[b]	*P. falciparum* (K1)[c]	*T. cruzi*[d]	*T. brucei rhodesiense*[e]	*L. donovani*[f]	L6 cells (cytotoxicity)[g]	selectivity index[h]
standard	0.008[i]	0.36[i]	3.6[j]	0.007[k]	0.43[l]	0.041[m]	—[h]
4a	6.3	1.6	73.4	9.8	170	9.1	5.6 (K1)
4b	4.9	1.4	122.8	7.8	53.4	20.9	15.0 (K1)
5	0.84	n.d.	102	9.4	>250	47.7	56.8 (NF54)
6	22.2	8.2	225	106	>250	>250	>30 (K1)

[a]The IC_{50} values are the means of two independent assays; the individual values vary by a factor of less than 2. [b]Chloroquine-sensitive strain of *P. falciparum*. [c]Chloroquine- and pyrimethamine-resistant strain of *P. falciparum*. [d]Tulahuen C4 strain of *T. cruzi* (amastigotes in L6 cells). [e]STIB 900 strain of *T. brucei rhodesiense* (trypomastigotes). [f]MHOM-ET-67/L82 strain of *L. donovani* (axenic amastigotes). [g]Mammalian host cells (rat skeletal myoblast L6 cells). [h]The selectivity index is calculated as the ratio of the IC_{50} values for the L6 cells to the IC_{50} data relative to *P. falciparum*. [i]Chloroquine. [j]Benznidazole. [k]Melarsoprol. [l]Miltefosine. [m]Podophyllotoxin.

analogue of **4a**, had the structure **8** (Figure 1); it was likewise new and was given the name ealamine F.

Ealamine G (9). The seventh new alkaloid was isolated from the twigs of *A. ealaensis*. It was obtained as an optically active yellowish powder. According to HRESIMS and NMR analysis, it had the same molecular formula of $C_{24}H_{27}NO_4$ as the above-described ealamine C (**5**) and the same constitution. From an NOE correlation between H-1 (δ_H 4.68) and H-3 (δ_H 3.49), the relative configuration at C-1 versus C-3 was deduced to be *cis* (see Supporting Information). The formation of *R*-3-aminobutyric acid in the oxidative degradation proved the new metabolite to be *R*-configured at C-3. Given the relative *cis*-configuration at C-1 and C-3 in the tetrahydroisoquinoline moiety, this indicated C-1 to be *S*-configured. NOESY interactions between Me-1 (δ_H 1.72) and H-1′ (δ_H 6.85), and between H-1 (δ_H 4.68) and H-7′ (δ_H 7.17), in conjunction with the *R*-configuration at C-3, etablished the biaryl axis to be *P*-configured. This was confirmed by the nearly identical ECD spectrum of the new alkaloid compared to that of the likewise *P*-configured ealamine A (**4a**) (see Supporting Information). As a consequence, the new compound had the stereostructure **9** as displayed in Figure 1. It was, hence, the 1,7-di-*epi*-analogue of the co-occurring ealamine C (**5**) and named ealamine G.

Ealamine H (10). A further new metabolite was isolated from the twig extract of *A. ealaensis*, again obtained as an optically active yellowish powder. As deduced by HRESIMS, it had a molecular formula of $C_{25}H_{29}NO_4$, identical to that of **4a**. Its ^{1}H (Table 2) and ^{13}C NMR (Table 3) spectra were very similar to those of ealamine E (**7**). The 2D NMR correlations indicated that the new metabolite possessed two methoxy groups at C-8 and C-5′ and—similar to **7**—an *N*-methyl group in the tetrahydroisoquinoline part, as evidenced by NOE correlations of the *N*-Me protons at δ_H 3.08 with the two methyl doublets of C-1 and C-3. From a NOE correlation between H-1 (δ_H 4.60) and H-3 (δ_H 3.47), the relative configuration of the methyl groups at C-1 versus C-3 was deduced to be *cis* (Figure 9A). The oxidative degradation procedure[35] afforded the *S*-enantiomer of *N*-methyl-3-amino-butyric acid, thus establishing the absolute configuration at C-3 as *S*, which, given the relative *cis*-configuration, determined the absolute configuration at C-1 to be *R*. On the basis of this absolute 1*R*,3*S*-stereoarray in the tetrahydroisoquinoline portion, in combination with the observed long-range NOESY cross-peaks between Me-1 (δ_H 1.75) and H-7′ (δ_H 7.19) and between H-1 (δ_H 4.60) and H-1′ (δ_H 6.74) (Figure 9A), the configuration at the axis was assigned as *P*. The axial *P*-configuration was confirmed by the ECD spectrum of the new metabolite, which was in accordance with that of the co-occurring—and likewise *P*-configured—ealamine A (**4a**) (Figure 9C). According to these findings, the new alkaloid had the stereostructure **10** as presented in Figure 1. It was, thus, the 3-*epi*-4′-*O*-demethyl analogue of ealamine E (**7**) and named ealamine H. With its *S*-configuration at C-3 and an oxygen function at C-6 it was a typical Ancistrocladaceae-type[1,3] compound. Within this series of ten 7,8′-linked naphthylisoquinolines presented here, only one of the other alkaloids isolated from *A. ealaensis* belonged to the subclass of Ancistrocladaceae-type metabolites, viz., the known[31,32] 6-*O*-demethylancistrobrevine A (**11**) (Figure 1), which had previously been discovered in two *Ancistrocladus* species from West and Central Africa.

DOI: 10.1021/acs.jnatprod.9b00755
J. Nat. Prod. 2019, 82, 3150−3164

Antiprotozoal Activities of Ealamines A–D (4a, 4b, 5, and 6). Some of the mono- and dimeric naphthylisoquinoline alkaloids previously discovered in *A. ealaensis* have been found to display promising antiprotozoal activities in vitro.[9−12] Most remarkable are the potent antileishmanial and antitrypanosomal effects[9] of the monomer ancistroealaine A (**2**) (Figure 1) and the antiplasmodial activities of the dimer ealapasamine C (**1**) (Figure 1) against the chloroquine-resistant K1 strain of *Plasmodium falciparum* (IC_{50} = 6.3 nM), combined with a very low cytotoxicity (IC_{50} = 6.0 μM), giving rise to a selectivity index (SI) of nearly 1000.[10] In view of these findings, the new ealamines A (**4a**), B (**4b**), C (**5**), and D (**6**) were likewise tested for their in vitro activities against the pathogens causing malaria (*Plasmodium falciparum*), Chagas' disease (*Trypanosoma cruzi*), human African sleeping sickness (*Trypanosoma brucei rhodesiense*), and visceral leishmaniasis (*Leishmania donovani*) (Table 4). Due to the lack of material, ealamines E–H (**6**–**10**) were not tested.

The most significant activities of the four new alkaloids were found against *P. falciparum* parasites. Noteworthy were the good inhibitory effects of the two atropo-diastereomers ealamines A (**4a**) and B (**4b**) against the K1 strain, though not reaching the extraordinary activity of the dimer ealapasamine C (**1**). Interestingly, the inhibitory potential of the atropisomeric alkaloids **4a** and **4b** against *Plasmodium* parasites showed comparable values, both against the chloroquine-sensitive NF54 strain, with IC_{50} values of 6.3 μM for **4a** and 4.9 μM for **4b**, and against the chloroquine-resistant K1 strain, with IC_{50} values of 1.6 μM for **4a** and 1.4 μM for **4b** (Table 4). All of the four tested alkaloids exerted only moderate cytotoxicities against rat skeletal myoblast (L6) cells, thus showing a structure-dependent specificity of their antiplasmodial activities (Table 4). The ealamines A–D (**4a**, **4b**, **5**, and **6**) exhibited only weak or virtually no antitrypanosomal or antileishmalial activities.

Preferential Cytotoxicity against PANC-1 Cells. Pancreatic cancer remains one of the leading causes of cancer-related mortality worldwide.[41] Since the disease is asymptomatic in the first phase, this aggressive malignancy is typically diagnosed only at an advanced stage, when most of the patients already suffer from enhanced metastases.[42] The rapid development of resistance to most conventional chemotherapeutic agents such as 5-fluorouracil and gemcitabine is one of the main reasons for treatment failure, leading to a poor prognosis and a low 5-year survival rate of less than 5%.[41,43] The development of anticancer drugs based on novel mechanisms for the pancreatic cancer treatment is thus urgently needed.[44]

The new ealamines A–D and G (**4a**, **4b**, **5**, **6**, and **9**) and the likewise 7,8′-coupled known[32] alkaloid yaoundamine A (**12**) were tested for their cytotoxic activities against the PANC-1 human pancreatic cancer cell line in normal, nutrient-rich medium (Dulbecco's modified Eagle's medium, DMEM) and in nutrient-deprived medium (NDM), following the antiausterity strategy.[45,46] This approach aims at the search for potent compounds for a targeted inhibition of the specific ability of pancreatic cancer cells to tolerate nutrient and oxygen deprivation. Human pancreatic cancer cells were found to be able to modulate their energy metabolism, thus allowing them to survive up to 72 h and proliferate even in the complete absence of essential nutrients such as glucose, amino acids, and serum.[46] Compounds displaying preferential cytotoxicity in NDM without exhibiting cytotoxicity in DMEM are therefore considered to be antiausterity agents.[18,46−49] The data in Table 5 are given as preferential cytotoxicity (PC_{50}) values, representing the concentrations of the investigated compounds at which 50% of the pancreatic cancer cells are killed in NDM without apparent toxicity in DMEM.

All of the 7,8′-coupled naphthylisoquinolines examined here displayed moderate to strong preferential cytotoxicities against PANC-1 cancer cells in a concentration-dependent manner, with PC_{50} values ranging from 9.9 to 60.4 μM (Table 5). Within this series of alkaloids, the two new ealamines A (**4a**) and C (**5**) were found to be the most potent representatives, with PC_{50} values of 12.5 and 9.9 μM, respectively (Figure 10), and thus exhibiting preferential cytotoxic activities comparable to those of the most active monomeric alkaloids previously discovered in related West and Central African species, yet belonging to the subgroups of 5,8′- or 5,1′-linked naphthylisoquinolines. The test results indicated that the degree of *O*-methylation in the naphthalene subunit may significantly affect the cytotoxic properties of the compounds, as seen from the only moderate antiausterity effect induced by ealamine B (**4b**) (PC_{50}, 30.6 μM) compared to the significantly stronger effect exerted by its 5′-*O*-demethyl analogue ealamine C (**5**) (PC_{50}, 9.9 μM). This tendency was also supported by the quite weak preferential cytotoxicity of ealamine D (**6**) (PC_{50}, 60.4 μM), equipped with two *O*-methyl groups in the naphthalene unit. The nearly similar PC_{50} values (33.4 and 37.8 μM) of ealamine G (**9**) and yaoundamine A (**12**) suggested that the degree of hydrogenation in the isoquinoline portion had no significant influence on the cytotoxicity of the compounds, whereas axial chirality seemed to be of crucial importance: Ealamine A (**4a**) (PC_{50}, 12.5 μM) exerted a much stronger cytotoxic effect toward PANC-1 cells than its atropo-diastereomer ealamine B (**4b**) (PC_{50}, 30.6 μM).

Table 5. Preferential Cytotoxicity of Ealamines A (4a) B (4b), C (5), D (6), and G (9) and Yaoundamine A (12) on Human Pancreatic Cancer PANC-1 Cells in NDM

compound	PC_{50} (in μM)[a]	compound	PC_{50} (in μM)[a]
4a	12.5	**9**	33.4
4b	30.6	**12**	37.8
5	9.9		
6	60.4	arctigenin[b]	0.8

[a]Concentration at which 50% of cells were killed preferentially in NDM. [b]Used as reference compound.

Ealamine C (**5**), as the most potent compound, was further investigated for its effects on cell morphology and apoptosis using the ethidium bromide (EB)–acridine orange (AO) double-staining fluorescence assay. AO and EB are both DNA intercalating dyes, but they differ in their ability to penetrate into the cell. While AO can easily pass the membrane, EB can penetrate only when the membrane integrity is lost during the cell death process. As such, the living cell emits the bright green fluorescence due to AO, whereas dead or dying cells emit predominantly red fluorescence due to EB. As shown in Figure 11, the morphology of human PANC-1 cells remained intact even when exposed to complete nutrient deprivation for 24 h and due to AO emitted green fluorescence exclusively. Treatment with ealamine C (**5**), on the other hand, resulted in a noticeable alteration of the PANC-1 cell morphology in a concentration-dependent manner. Treatment with 12.5 μM ealamine C (**5**) led to both EB- and AO-stained cells,

DOI: 10.1021/acs.jnatprod.9b00755
J. Nat. Prod. 2019, 82, 3150−3164

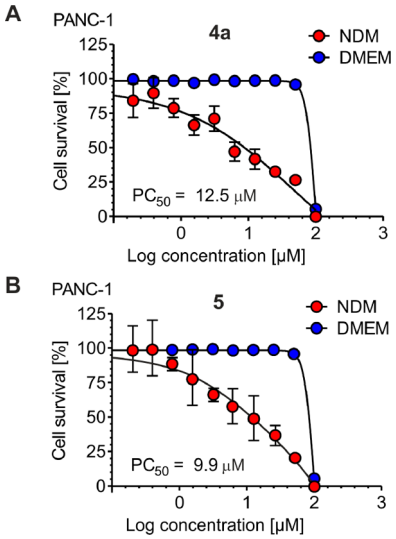

Figure 10. Preferential cytotoxic activities of ealamines A (**4a**) (A) and C (**5**) (B) against the PANC-1 human pancreatic cancer cell line in nutrient-deprived medium (NDM) and Dulbecco's modified Eagle's medium (DMEM).

suggesting the loss of membrane integrity and cell death processes. However, addition of 25 μM **5** caused a complete swelling and rounding of PANC-1 cell morphology, giving rise to red fluorescence exclusively. All this evidence suggested that ealamine C (**5**) is a promising antiausterity agent having the ability to kill PANC-1 human pancreatic cancer cells preferentially under nutrition starvation conditions.

Concluding Remarks. In summary, an unusually broad series of ten 7,8′-coupled naphthylisoquinoline alkaloids were discovered in the leaves and twigs of the Central African liana *A. ealaensis*, among them eight new compounds, ealamines A–H (**4a**, **4b**, and **5**–**10**), all of them oxygenated at C-6. While only one of the new compounds, ealamine H (**10**), was a typical Ancistrocladaceae-type metabolite, i.e., with *S*-configuration at C-3, seven of them represented the first 7,8′-linked naphthyltetrahydroisoquinolines with *R*-configuration at C-3, thus belonging to the mixed Ancistrocladaceae/Dioncophyllaceae-hybrid type. The elucidation of the absolute axial configuration of the latter turned out be unexpectedly challenging due to their unprecedented conformational behavior and required selective and time-demanding NOESY experiments with mixing-time optimization. The NOE cross-peak between Me-1 and Me-2′ was recognized to be the one decisive for a reliable identification of 7,8′-coupled hybrid-type alkaloids with an *M*-configuration at the axis. This is based on the fact that the energetically preferred conformers of 7,8′-coupled alkaloids with the combination *M*-configuration at the axis and *R* at C-3—and, in particular if equipped with a shielding methoxy group at C-8 like ealamine B (**4b**)—were found to adopt a conformational arrangement of the tetrahydropyrido ring system with both the nitrogen atom and C-3 being located "up", and not, as in other investigated cases,[6,19] occupying a half-chair array. These structural pecularities were confirmed by DFT calculations of the minimum structures of the new ealamines.

Remarkably, the decisive Cotton effects displayed by 7,8′-coupled naphthylisoquinolines were weaker than those exerted in 5,8′-coupled alkaloids, in particular in the case of the *P*-configured compounds, which showed very small positive Cotton effects around 220 nm. This weak ECD effect now explained why in the case of the mixed-coupled dimers, such as, ealapasamine C (**1**) (Figure 1), which consist of a 5,8′- and a 7,8′-linked monomeric half, the overall ECD spectra were always dominated by the strong effects of the korupensamine-like, 5,8′-coupled moieties.[10] Another highlight of this study is the X-ray structure analysis of ealamine A (**4a**), which is one of the few examples of naphthylisoquinoline alkaloid crystal

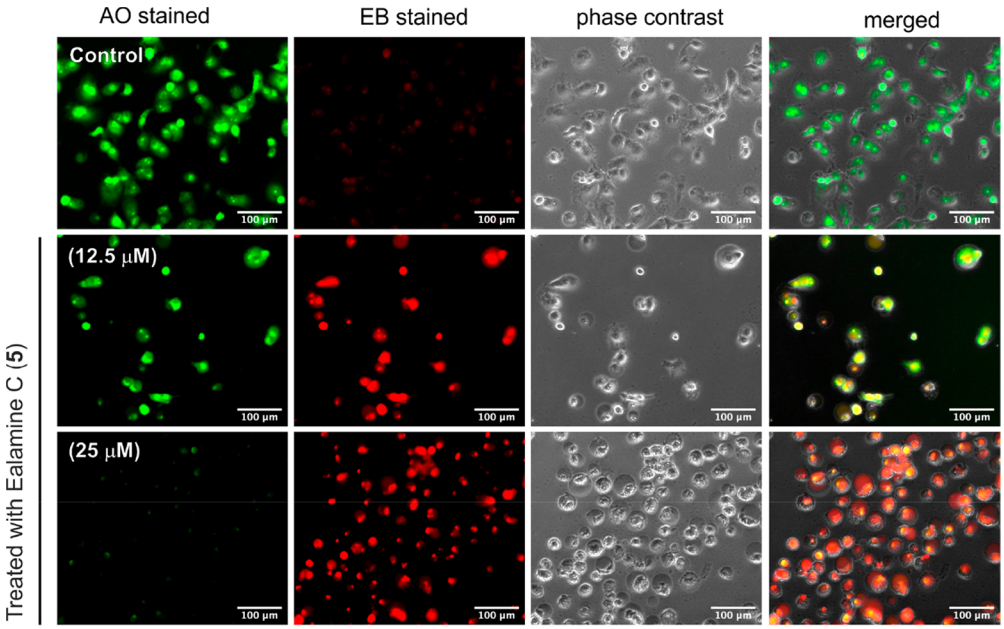

Figure 11. Morphological changes of PANC-1 cells induced by ealamine C (**5**) in comparison to untreated cells (i.e., the control) in nutrient-deprived medium (NDM). PANC-1 tumor cells were treated with **5** at the indicated concentrations in NDM and incubated for 24 h. Cells were stained with ethidium bromide (EB) and acridine orange (AO) and photographed under fluorescence (red and green) and phase contrast (gray) modes using an EVOS FL digital microscope.

DOI: 10.1021/acs.jnatprod.9b00755
J. Nat. Prod. 2019, 82, 3150–3164

structures and even the very first one for a 7,8′-linked representative.

In many African and Asian *Ancistrocladus* species, mono- and dimeric alkaloids with 5,8′-, 5,1′-, or 7,1′-biaryl linkages had so far been found to dominate the metabolite profiles,[1−3,9,11−18,20,21,24−29] whereas 7,8′-coupled naphthylisoquinolines had only rarely been identified, and if so, mainly occurring as minor metabolites.[1,3,6,10,19,23,30−33]

The discovery of such a large series of alkaloids with the otherwise so scarce 7,8′-coupling type in *A. ealaensis* demonstrates that this Central African liana occupies an outstanding chemo- and geotaxonomic position within the genus *Ancistrocladus*. This is also underlined by the special ability of *A. ealaensis* to synthesize constitutionally unsymmetric heterodimers like the ealapasamines A−C.[10] Only the Cameroonian species *A. korupensis* has so far been reported to produce another mixed dimer with a related molecular scaffold, viz., korundamine A,[33] along with two 7,8′-coupled hybrid-type monomers, yaoundamine A (**12**) and its 6-*O*-L-rhamnoside analogue, named yaoundamine B.[32]

Furthermore, *A. ealaensis* has now become a promising source of potent bioactive compounds, with interesting antiprotozoal,[9−12] antileukemic,[11] and, as presented here, also promising preferential cytotoxic activities against PANC-1 human cancer cells. All these results warrant further studies on the pharmacological potential of naphthylisoquinoline alkaloids in general. This work is currently in progress.

EXPERIMENTAL SECTION

General Experimental Procedures. Optical rotations were determined on a JASCO P-1020-polarimeter, UV spectra were determined on a Shimadzu UV-1800 spectrophotometer, and ECD measurements were performed under nitrogen on a JASCO J-715 spectrometer at room temperature, using spectrophotometric-grade methanol. The ECD data were processed using SpecDis.[50] 1D and 2D NMR spectra were monitored on Bruker AMX 400 and DMX 600 instruments, using methanol-d_4 (δ_H 3.31 and δ_C 49.15 ppm) as the solvent. Chemical shifts (δ) are reported in parts per million (ppm), and coupling constants (J) are given in hertz (Hz). NMR signal multiplicities are denoted as singlet (s), doublet (d), doublet of doublets (dd), quartet (q), pseudoquartet (pq), or multiplet (m). Spectra were acquired and processed using an ACD/NMR processor (version 12.01) and the Topspin 3.2 software (Bruker Daltonics). HRESIMS measurements were performed in positive mode on a Bruker Daltonics micrOTOF-focus mass instrument. HPLC-DAD investigations were conducted on a JASCO LC-2000 Plus series system. For LC-MS analysis, an Agilent 1100 series system was used, equipped with a binary high-pressure mixing pump, with a degasser module, an autosampler, a 1100 series photodiode array (PDA) detector (Agilent Technology), and an Esquire 3000 Plus ion-trap mass spectrometer with an electrospray ionization interface (Bruker Daltonics). GC-MSD was performed on a GCMS-QP 2010SE system (Shimadzu). Preparative HPLC was carried out on a JASCO system (PU-1580 Plus) in combination with UV/vis detection at 200−680 nm (JASCO MD-2010 Plus diode array detector) at room temperature. For maceration, a mechanical shaker was used at 160 rpm (rotations per minute). All organic solvents were of analytical-grade quality. Ultrapure water was obtained from an Elga Purelab Classicsystem. (*S*)-MTPA was purchased from Sigma-Aldrich (Steinheim, Germany).

Plant Material. Twigs and leaves of *Ancistrocladus ealaensis* J. Léonard[7,8] were collected at Eala Botanical Garden (Jardin Botanique d'Eala, Mbandaka, Democratic Republic of the Congo) in August 2008 by one of us (V.M.), and in August 2015 by Mr. B. K. Lombe (GPS coordinates 00°03.605 N, 018°.886 E). The material of 2015 was additionally authenticated by LC-DAD-MS to contain the same metabolites as the one of 2008. Voucher specimens (Nos. 43 and 57) have been deposited at the Herbarium Bringmann, University of Würzburg.

Extraction and Isolation. Following a protocol described previously,[11] naphthylisoquinoline alkaloids were extracted from air-dried leaves (600 g) by repeated maceration of the fine-powdered plant material in MeOH (four cycles of 24 h each) to give, after removal of the solvent, a viscous solution. The extract was dissolved in water and cleared from chlorophyll by extracting with *n*-hexane. Liquid/liquid partitioning between water and CH_2Cl_2 provided an alkaloid-enriched fraction (5.1 g), which was subjected to column chromatography (CC) on C_{18} reversed-phase silica gel using a gradient (0:50 → 50:0) of CH_3CN and ultrapure water containing 0.05% TFA. Fractions F_{12} to F_{35} were further resolved on five Sep-Pak C_{18} Plus Light cartridges coupled in series (adsorbent: 130 mg, particle size: 55−105 μm), again using a gradient of CH_3CN and ultrapure water from 0 to 50% H_2O in CH_3CN.

Assisted by LC-MS and LC-UV analysis to search for metabolites of interest, alkaloid-containing subfractions were subjected to HPLC on a SymmetryPrep C_{18} column, 19 × 300 mm, 7 μm (Waters), using a solvent system consisting of A (H_2O, 0.05% TFA) and B (CH_3CN, 0.05% TFA), with a linear gradient (0−12 min: 10−20% B, 35 min: 45% B, 37 min: 50% B, 40 min: 100% B, 44 min: 100% B), at a flow rate of 10 mL min^{-1}. Further purification of the collected compounds was achieved by HPLC on a Chromolith SemiPrep RP-18e column, 100 × 10 mm (Merck), by applying the following gradient at a flow rate of 10 mL min^{-1}: A (H_2O, 0.05% TFA) and C (MeOH, 0.05% TFA): 0−2 min: 10% C, 8 min: 30% C, 11 min: 35% C, 20 min: 40% C, 25 min: 45% C, 27 min: 100% C, to afford 18.5 mg of ealamine A (**4a**) (retention time 11.1 min), 10.3 mg of ealamine B (**4b**) (retention time 10.8 min), 11.1 mg of ealamine C (**5**) (retention time 13.2 min), 4.0 mg of ealamine D (**6**) (retention time 11.7 min), and 0.9 mg of ealamine E (**7**) (retention time 12.5 min). Two further alkaloid-containing subfractions were resolved similarly, by preparative HPLC on a SymmetryPrep C_{18} column, using a linear gradient solvent system consisting of A and B (0−5 min: 15% B, 6 min: 20% B, 20 min: 25% B, 30 min: 30% B, 37 min: 55% B), at a flow rate of 10 mL min^{-1}. Additional purification steps of the collected compounds were performed on a Chromolith SemiPrep RP-18e column, using a linear gradient of solvents A and C: 30% C, 13 min: 40% C, 19 min: 55% C, 20 min: 100% C, 23 min: 100% C, at a flow rate of 10 mL min^{-1}, to yield 0.7 mg of ealamine F (**8**) (retention time 12.9 min) and 1.2 mg of yaoundamine A (**12**) (retention time 15.2 min).

Following a protocol described previously,[11] fine-powdered material of air-dried twigs (ca. 300 g) of *A. ealaensis* was exhaustively extracted with MeOH/CH_2Cl_2 (7:3) at room temperature to give 2.8 g of a crude residue, which was, after dissolution in MeOH/water, subjected to liquid−liquid partition with *n*-hexane to remove nonpolar compounds. CC on silica gel (deactivated with triethylamine) using a gradient of CH_2Cl_2 and MeOH (80:20 → 20:80) afforded several alkaloid-containing subfractions, which were further resolved by preparative reversed-phase HPLC on a SymmetryPrep C_{18} column with a solvent system consisting of A (MeOH, 0.05% TFA) and B (CH_3CN, 0.05% TFA). Using a linear gradient (0−10 min 18% B, 13−25 min 20% B, 45 min 50% B, 48 min 100% B) at a flow rate of 20 mL min^{-1}, 5.3 mg of ealamine G (**9**) (retention time 21.3 min), 3.1 mg of ealamine H (**10**) (retention time 19.6 min), and 3.4 mg of 6-*O*-demethylancistrobrevine A (**11**) (retention time 25.1 min) were obtained, along with 4.2 mg of yaoundamine A (**12**) (retention time 31.3 min) and 10.0 mg of ealamine A (**4a**) (retention time 22.5 min).

*Ealamine A (**4a**):* brownish, amorphous powder; $[\alpha]_D^{23}$ −15.0 (*c* 0.05, MeOH); UV (MeOH) λ_{max} (log ε) 200 (5.9), 203 (6.9), 219 (4.6), 231 (5.6), 265 (0.5), 307 (1.2), 321 (1.0), 350 (0.2) nm; ECD (*c* 0.10; MeOH) λ_{max} (log ε) 213 (−13.3), 225 (+3.8), 236 (−1.5), 240 (+0.1), 244 (−0.4), 257 (+8.4), 284 (−7.3), 318 (+2.1), 322 (+2.1) nm; ^{1}H NMR and ^{13}C NMR see Table 1; HRESIMS *m*/*z* 408.21570 $[M + H]^+$ (calcd for $C_{25}H_{30}NO_4$, 408.21693).

*Ealamine B (**4b**):* yellowish, amorphous powder; $[\alpha]_D^{23}$ −15.0 (*c* 0.04, MeOH); UV (MeOH) λ_{max} (log ε) 200 (4.1), 206 (4.6), 218

DOI: 10.1021/acs.jnatprod.9b00755
J. Nat. Prod. 2019, 82, 3150−3164

(3.6), 231 (4.7), 265 (0.4), 307 (1.1), 321 (0.9), 350 (0.01) nm; ECD (*c* 0.10, MeOH) λ_{max} (log ε) 200 (+10.4), 214 (−8.6), 225 (−11.5), 230 (−15.6), 241 (0.0), 251 (+3.8), 284 (−3.5), 311 (+1.7), 349 (−0.7), 360 (+0.1) nm; ^{1}H NMR and ^{13}C NMR, see Table 1; HRESIMS *m*/*z* 408.21610 $[M + H]^+$ (calcd for $C_{25}H_{30}NO_4$, 408.21693).

*Ealamine C (**5**):* brownish, amorphous powder; $[\alpha]_D^{23}$ −24.0 (*c* 0.07, MeOH); UV (MeOH) λ_{max} (log ε) 200 (5.4), 205 (6.9), 218 (5.3), 231 (7.1), 260 (0.5), 307 (1.3), 321 (1.2), 333 (0.8), 350 (0.01) nm; ECD (*c* 0.20, MeOH) λ_{max} (log ε) 200 (−25.6), 203 (−59.4), 215 8 + 7.6), 217 (−25.1), 222 (+1.7), 227 (−79.9), 232 (+8.1), 252 (+15.4), 285 (−9.3), 315 (+6.1), 360 (+0.5) nm; ^{1}H NMR and ^{13}C NMR, see Tables 2 and 3; HRESIMS *m*/*z* 394.20194 $[M + H]^+$ (calcd for $C_{24}H_{28}NO_4$, 394.20128).

*Ealamine D (**6**):* yellowish, amorphous powder; $[\alpha]_D^{23}$ −17.0 (*c* 0.06, MeOH); UV (MeOH) λ_{max} (log ε) 200 (6.0), 205 (6.4), 218 (5.0), 227 (4.8), 271 (1.3), 288 (1.1), 307 (1.1), 350 (0.4) nm; ECD (*c* 0.01, MeOH) λ_{max} (log ε) 200 (+4.9), 215 (−5.1), 219 (−5.9), 224 (−3.5), 232 (−5.9), 242 (+0.03), 247 (+0.8), 267 (−1.2), 287 (+0.2), 303 (−0.2), 314 (+0.7), 323 (+0.3), 332 (+0.7), 360 (−0.2) nm; ^{1}H NMR and ^{13}C NMR, see Tables 2 and 3; HRESIMS *m*/*z* 408.21610 $[M + H]^+$ (calcd for $C_{25}H_{30}NO_4$, 408.21693).

*Ealamine E (**7**):* yellowish, amorphous powder; $[\alpha]_D^{23}$ −13.0 (*c* 0.02, MeOH); UV (MeOH) λ_{max} (log ε) 200 (4.2), 205 (5.9), 218 (5.1), 231 (6.3), 260 (0.1), 307 (1.2), 321 (1.0), 333 (0.3) nm; ECD (*c* 0.02, MeOH) λ_{max} (log ε) 200 (+2.5), 211 (−0.2), 215 (+0.3), 233 (−1.5), 251 (+0.2), 284 (−1.3), 311 (+0.3), 323 (+0.3), 348 (+0.2) nm; ^{1}H NMR and ^{13}C NMR, see Tables 2 and 3; HRESIMS *m*/*z* 422.23295 $[M + H]^+$ (calcd for $C_{26}H_{32}NO_4$, 422.23303).

*Ealamine F (**8**):* yellow, amorphous powder; $[\alpha]_D^{23}$ −15.0 (*c* 0.04, MeOH); UV (MeOH) λ_{max} (log ε) 200 (4.1), 206 (5.9), 217 (4.8), 230 (5.8), 261 (0.2), 307 (1.1), 321 (1.0), 333 (0.2) nm; ECD (*c* 0.06, MeOH) λ_{max} (log ε) 200 (+9.8), 211 (−4.7), 219 (+2.9), 233 (−1.8), 242 (−0.3), 261 (−3.1), 310 (+0.4), 318 (+0.5), 352 (−0.3), 365 (−0.3) nm; ^{1}H NMR and ^{13}C NMR, see Tables 2 and 3; HRESIMS *m*/*z* 422.23356 $[M + H]^+$ (calcd for $C_{26}H_{32}NO_4$, 422.23303).

*Ealamine G (**9**):* yellowish, amorphous powder; $[\alpha]_D^{23}$ −20.0 (*c* 0.08, MeOH); UV (MeOH) λ_{max} (log ε) 200 (3.4), 205 (6.9), 218 (5.3), 231 (7.1), 260 (0.5), 307 (1.3), 321 (1.2), 333 (0.8), 350 (0.01) nm; ECD (*c* 0.09, MeOH) λ_{max} (log ε) 200 (+1.07), 204 (−8.46), 210 (+8.32), 212 (+5.51), 213 (+8.15), 216 (+4.45), 221 (+9.58), 234 (−1.55), 257 (+21.07), 286 (−12.70), 335 (+0.24), 400 (0.0) nm; ^{1}H NMR and ^{13}C NMR, see Tables 2 and 3; HRESIMS *m*/*z* 394.20180 $[M + H]^+$ (calcd for $C_{24}H_{28}NO_4$, 394.20128).

*Ealamine H (**10**):* yellowish, amorphous powder; $[\alpha]_D^{23}$ −14.0 (*c* 0.02, MeOH); UV (MeOH) λ_{max} (log ε) 200 (2.3), 205 (5.3), 218 (5.2), 231 (8.1), 260 (0.3), 307 (1.3), 321 (1.2), 333 (0.8), 350 (0.01) nm; ECD (*c* 0.09, MeOH) λ_{max} (log ε) 200 (+3.59), 207 (+2.57), 216 (+0.53), 224 (+1.41), 228 (+0.82), 235 (+0.75), 254 (+5.84), 283 (−5.63), 310 (+0.66), 337 (−0.24), 381 (−0.20) nm; ^{1}H NMR and ^{13}C NMR, see Tables 2 and 3; HRESIMS *m*/*z* 408.21640 $[M + H]^+$ (calcd for $C_{25}H_{30}NO_4$, 408.21693).

Oxidative Degradation. Ruthenium(VIII)-catalyzed periodate degradation of ealamines A−H (**4a**, **4b**, and **5**−**10**), the derivatization of the resulting amino acids, and the assignment of the absolute configurations of **4a**, **4b**, and **5**−**10** in their tetrahydroisoquinoline subunits by GC-MSD analysis were carried out following a protocol developed earlier.[35]

X-ray Crystallographic Analysis of Ealamine A (4a). Single crystals suitable for structural analysis were obtained by slow, gentle diffusion of *n*-hexane into a solution of **4a** in acetone at room temperature in the presence of trifluoroacetic acid. The crystal data of **4a** in its protonated form were collected at *T* = 100 K on a Bruker D8 Quest Kappa diffractometer using a Photon 100 CMOS detector and multilayer mirror monochromated Cu Kα radiation (λ = 1.541 84 Å). The structure was solved using direct methods, refined with the SHELXL software package,[51] and expanded using Fourier techniques. All non-hydrogen atoms were refined anisotropically. Hydrogen atoms were included in the calculations of the structural factors and assigned to idealized geometric positions. Crystallographic data for **4a** have been deposited with the Cambridge Crystallographic Data Centre (deposition number: CCDC 1939956). Copies of these data can be obtained, free of charge, from the Cambridge Crystallographic Data Centre via www.ccdc.cam.ac.uk/data_request/cif.

*Crystal data of **4a**:* (2 $C_{27}H_{30}NO_6F_3 \cdot C_3H_6O$), M_r = 1101.12, crystal size 0.463 × 0.424 × 0.285 mm^3, triclinic space group *P*1, *a* = 8.9167(7) Å, *b* = 11.8688(12) Å, *c* = 14.7500(15) Å, α = 68.987(6)°, β = 73.430(7)°, γ = 77.232(7)°, *V* = 1384.3(2) Å^3, *Z* = 1, ρ_{calcd} = 1.321 g cm^{-3}, μ = 0.900 mm^{-1}, *F*(000) = 580, *T* = 100(2) K, GooF(F^2) = 1.051, R_1 = 0.0277, wR_2 = 0.0744 for $I > 2\sigma(I)$, R_1 = 0.0278, wR_2 = 0.0745 for all data, 10 743 unique reflections [$\theta \leq$ 74.538°] with a completeness of 99.9% and 725 parameters, 3 restraints, Flack parameter, *x* = 0.053(13).

Computational Details. The computational ECD analysis has been done as described in the literature.[52] B3LYP-D3/def2-SVP[53] conformational analyses and CAM-B3LYP/def2-TZVP(-f) TD calculations were performed using ORCA 3.0[40] making use of the chain-of-sphere approximation (RIJCOSX)[54] and in the case of the TD calculation the COSMO(methanol) keyword. Evaluation of the results was done using SpecDis 1.71[50] with a σ of 0.2 eV and a UV shift of 25 nm for ealamine A (**4a**) and of 22 nm for ealamine B (**4b**).

Antiprotozoal Evaluation. Antiparasitic activities and cytotoxicities of ealamines A (**4a**), B (**4b**), C (**5**), and D (**6**) (Table 4) were determined in vitro according to well-established protocols, as reported previously.[55]

Preferential Cytotoxicity Assay against PANC-1 Cells. The ealamines A−D (**4a**, **4b**, **5**, and **6**) (Table 5) were evaluated for their preferential cytotoxicity against PANC-1 human pancreatic cancer cells (RBRC-RCB2095 purchased from the Riken BRC cell bank) by a procedure described previously.[18,44,56]

Morphological Assessment of Cancer Cells after Treatment with Ealamine C (5). Following a protocol published earlier,[18,20,44] PANC-1 cells were treated for 24 h with ealamine C (**5**) at different concentrations or without any agent (control) in NDM. Cell morphology (Figure 11) was visualized after addition of EB/AO using an EVOS FL digital microscope (20× objective).

■ ASSOCIATED CONTENT

Supporting Information

The Supporting Information is available free of charge on the ACS Publications website at DOI: 10.1021/acs.jnatprod.9b00755.

NMR (^{1}H, ^{13}C, ^{1}H, ^{1}H−COSY, HSQC, HMBC, NOESY, and ROESY), HRESIMS, UV, and ECD spectra and GC-MSD chromatograms obtained from the oxidative degradation of **4a**, **4b**, and **5**−**10** (PDF)

X-ray crystallography data for **4a** (CIF)

■ AUTHOR INFORMATION

Corresponding Authors

*E-mail (S. Awale): suresh@inm.u-toyama.ac.jp. Tel: +81-76-434-7640. Fax: +81-76-434-7640.

*E-mail (G. Bringmann): bringman@chemie.uni-wuerzburg.de. Tel: +49-931-318-5323. Fax: +49-931-318-4755.

ORCID

Torsten Bruhn: 0000-0002-9604-1004

Frank Würthner: 0000-0001-7245-0471

Suresh Awale: 0000-0002-5299-193X

Gerhard Bringmann: 0000-0002-3583-5935

Notes

The authors declare no competing financial interest.

DOI: 10.1021/acs.jnatprod.9b00755
J. Nat. Prod. 2019, 82, 3150−3164

■ ACKNOWLEDGMENTS

This work was supported by the Deutsche Forschungsgemeinschaft (SFB 630, "Agents against Infectious Diseases", project A2) and by the German Excellence Initiative to the Graduate School of Life Sciences, University of Würzburg (grant to D.T.T.). Generous support from the Else-Kröner-Fresenius-Stiftung is also acknowledged. The biological evaluation against cancer cell lines was supported by the Japanese Society for the Promotion of Science (JSPS), Japan, Kakenhi (16K08319) to S.A. The authors thank Mrs. M. Michel for the degradation experiments and Mr. B. K. Lombe for the collection of additional leaf material of *A. ealaensis* in the Eala Botanical Garden (Jardin Botanique d'Eala, Province Équateur, DR Congo). Further thanks are due to Dr. M. Grüne and Mrs. Altenberger for the 600 MHz NMR measurements, to Mrs. J. Adelmann for the HRESIMS analyses, and to Mrs. A.-M. Krause for the ORTEP plot of ealamine A (all from the University of Würzburg). We also thank Mrs. M. Cal, Mrs. S. Keller-Märki, and Mrs. R. Rocchetti for help with the parasitic assays.

■ REFERENCES

(1) Lombe, B. K.; Feineis, D.; Bringmann, G. *Nat. Prod. Rep.* **2019**, DOI: 10.1039/C9NP00024K.

(2) (a) Bringmann, G.; Günther, C.; Ochse, M.; Schupp, O.; Tasler, S. In *Progress in the Chemistry of Organic Natural Products*; Herz, W.; Falk, H.; Kirby, G. W.; Moore, R. E., Eds.; Springer: Wien, NY, 2001; Vol. *82*, pp 111−123. (b) Bringmann, G.; François, G.; Aké Assi, L.; Schlauer, J. *Chimia* **1998**, *52*, 18−28. (c) Ibrahim, S. R. M.; Mohamed, G. A. *Fitoterapia* **2015**, *106*, 194−225.

(3) Bringmann, G.; Pokorny, F. In *The Alkaloids*; Cordell, G. A., Ed.; Academic Press: New York, 1995; Vol. *46*, Chapter 4, pp 127−271.

(4) (a) Kutchan, T. M.; Dittrich, H.; Bracher, D.; Zenk, M. H. *Tetrahedron* **1991**, *47*, 5945−5954. (b) Dewick, P. M. *Medicinal Natural Products*; Wiley-VCH: Weinheim, 2002; pp 315−326. (c) O'Connor, S. E. In *Natural Products in Chemical Biology*; Civjan, N., Ed.; John Wiley & Sons, Inc.: Hoboken, NJ, 2012; pp 209−237.

(5) (a) Bringmann, G.; Wohlfarth, M.; Rischer, H.; Grüne, M.; Schlauer, J. *Angew. Chem., Int. Ed.* **2000**, *39*, 1464−1466. (b) Bringmann, G.; Mutanyatta-Comar, J.; Greb, M.; Rüdenauer, S.; Noll, T. F.; Irmer, A. *Tetrahedron* **2007**, *63*, 1755−1761.

(6) Bringmann, G.; Irmer, A.; Rüdenauer, S.; Mutanyatta-Comar, J.; Seupel, R.; Feineis, D. *Tetrahedron* **2016**, *72*, 2906−2912.

(7) (a) Cheek, M. *Kew Bull.* **2000**, *55*, 871−882. (b) Taylor, C. M.; Gereau, R. E.; Walters, G. M. *Ann. Missouri Bot. Gard.* **2005**, *92*, 360−399.

(8) (a) Léonard, J. *Bull. Soc. R. Bot. Belg.* **1949**, *82*, 27−40. (b) Léonard, J. In *Flore D'Afrique Centrale (Zaïre - Rwanda - Burundi)*; Bamps, P., Ed.; Jardin Botanique National de Belgique: Meise, 1982.

(9) Bringmann, G.; Hamm, A.; Günther, C.; Michel, M.; Brun, R.; Mudogo, V. *J. Nat. Prod.* **2000**, *63*, 1465−1470.

(10) Tshitenge, D. T.; Feineis, D.; Mudogo, V.; Kaiser, M.; Brun, R.; Bringmann, G. *Sci. Rep.* **2017**, *7*, 5767.

(11) Tshitenge, D. T.; Feineis, D.; Mudogo, V.; Kaiser, M.; Brun, R.; Seo, E.-J.; Efferth, T.; Bringmann, G. *J. Nat. Prod.* **2018**, *81*, 918−933.

(12) Tshitenge, D. T.; Bruhn, T.; Feineis, D.; Mudogo, V.; Kaiser, M.; Brun, R.; Bringmann, G. *Sci. Rep.* **2019**, *9*, 9812.

(13) Bringmann, G.; Messer, K.; Brun, R.; Mudogo, V. *J. Nat. Prod.* **2002**, *65*, 1096−1101.

(14) Bringmann, G.; Steinert, C.; Feineis, D.; Mudogo, V.; Betzin, J.; Scheller, C. *Phytochemistry* **2016**, *128*, 71−81.

(15) Bringmann, G.; Günther, C.; Saeb, W.; Mies, J.; Wickramasinghe, A.; Mudogo, V.; Brun, R. *J. Nat. Prod.* **2000**, *63*, 1333−1337.

(16) Fayez, S.; Feineis, D.; Mudogo, V.; Awale, S.; Bringmann, G. *RSC Adv.* **2017**, *7*, 53740−53751.

(17) Fayez, S.; Feineis, D.; Mudogo, V.; Seo, E.-J.; Efferth, T.; Bringmann, G. *Fitoterapia* **2018**, *129*, 114−125.

(18) Awale, S.; Dibwe, D. F.; Balachandran, C.; Fayez, S.; Feineis, D.; Lombe, B. K.; Bringmann, G. *J. Nat. Prod.* **2018**, *81*, 2282−2291.

(19) Li, J.; Seupel, R.; Feineis, D.; Mudogo, V.; Kaiser, M.; Brun, R.; Brünnert, D.; Chatterjee, M.; Seo, E.-J.; Efferth, T.; Bringmann, G. *J. Nat. Prod.* **2017**, *80*, 443−458.

(20) Li, J.; Seupel, R.; Bruhn, T.; Feineis, D.; Kaiser, M.; Brun, R.; Mudogo, V.; Awale, S.; Bringmann, G. *J. Nat. Prod.* **2017**, *80*, 2807−2817.

(21) Bringmann, G.; Zhang, G.; Büttner, T.; Bauckmann, G.; Kupfer, T.; Braunschweig, H.; Brun, R.; Mudogo, V. *Chem. - Eur. J.* **2013**, *19*, 916−923.

(22) Bringmann, G.; Kajahn, I.; Reichert, M.; Pedersen, S. E. H.; Faber, J. H.; Gulder, T.; Brun, R.; Christensen, S. B.; Ponte-Sucre, A.; Moll, H.; Heubl, G.; Mudogo, V. *J. Org. Chem.* **2006**, *71*, 9348−9356.

(23) Bringmann, G.; Spuziak, J.; Faber, J. H.; Gulder, T.; Kajahn, I.; Dreyer, M.; Heubl, G.; Brun, R.; Mudogo, V. *Phytochemistry* **2008**, *69*, 1065−1075.

(24) (a) Bringmann, G.; Lombe, B. K.; Steinert, C.; Ndjoko Ioset, K.; Brun, R.; Turini, F.; Heubl, G.; Mudogo, V. *Org. Lett.* **2013**, *15*, 2590−2593. (b) Lombe, B. K.; Bruhn, T.; Feineis, D.; Mudogo, V.; Brun, R.; Bringmann, G. *Org. Lett.* **2017**, *19*, 1342−1345. (c) Lombe, B. K.; Bruhn, T.; Feineis, D.; Mudogo, V.; Brun, R.; Bringmann, G. *Org. Lett.* **2017**, *19*, 6740−6743.

(25) Lombe, B. K.; Feineis, D.; Mudogo, V.; Brun, R.; Awale, S.; Bringmann, G. *RSC Adv.* **2018**, *8*, 5243−5254.

(26) Kavatsurwa, S. M.; Lombe, B. K.; Feineis, D.; Dibwe, D. F.; Maharaj, V.; Awale, S.; Bringmann, G. *Fitoterapia* **2018**, *130*, 6−16.

(27) Mufusama, J.-P.; Feineis, D.; Mudogo, V.; Kaiser, M.; Brun, R.; Bringmann, G. *RSC Adv.* **2019**, *9*, 12034−12046.

(28) Hallock, Y. F.; Manfredi, K. P.; Blunt, J. W.; Cardellina CC, J. H.; Schäffer, M.; Gulden, K.-P.; Bringmann, G.; Lee, A. Y.; Clardy, J.; François, G.; Boyd, M. R. *J. Org. Chem.* **1994**, *59*, 6349−6355.

(29) (a) Boyd, M. R.; Hallock, Y. F.; Cardellina, J. H.; Manfredi, K. P.; Blunt, J. W.; McMahon, J. B.; Buckheit, R. W., Jr.; Bringmann, G.; Schäffer, M.; Cragg, G. M.; Thomas, D. W.; Jato, J. G. *J. Med. Chem.* **1994**, *37*, 1740−1745. (b) Hallock, Y. F.; Manfredi, K. P.; Dai, J. R.; Cardellina II, J. H.; Gulakowski, R. J.; McMahon, J. B.; Schäffer, M.; Stahl, M.; Gulden, K. P.; Bringmann, G.; François, G.; Boyd, M. R. *J. Nat. Prod.* **1997**, *60*, 677−683.

(30) (a) Bringmann, G.; Wohlfarth, M.; Rischer, H.; Schlauer, J.; Brun, R. *Phytochemistry* **2002**, *61*, 195−204. (b) Bringmann, G.; Zhang, G.; Ölschläger, T.; Stich, A.; Wu, J.; Chatterjee, M.; Brun, R. *Phytochemistry* **2013**, *91*, 220−228. (c) Bringmann, G.; Koppler, D.; Wiesen, B.; François, G.; Sankara Narayanan, A. S.; Almeida, M. R.; Schneider, H.; Zimmermann, U. *Phytochemistry* **1996**, *43*, 1405−1410. (d) Bringmann, G.; Dreyer, M.; Kopff, H.; Rischer, H.; Wohlfarth, M.; Hadi, H. A.; Brun, R.; Meimberg, H.; Heubl, G. *J. Nat. Prod.* **2005**, *68*, 686−690.

(31) Fayez, S.; Feineis, D.; Aké Assi, L.; Kaiser, M.; Brun, R.; Awale, S.; Bringmann, G. *Fitoterapia* **2018**, *131*, 245−259.

(32) (a) Bringmann, G.; Stahl, M.; Gulden, K.-P. *Tetrahedron* **1997**, *53*, 2817−2822. (b) Hallock, Y. F.; Cardellina II, J. H.; Schäffer, M.; Stahl, M.; Bringmann, G.; François, G.; Boyd, M. R. *Tetrahedron* **1997**, *53*, 8121−8128.

(33) Hallock, Y. F.; Cardellina II, J. H.; Schäffer, M.; Bringmann, G.; François, G.; Boyd, M. R. *Bioorg. Med. Chem. Lett.* **1998**, *8*, 1729−1734.

(34) Bringmann, G.; Wohlfarth, M.; Rischer, H.; Heubes, M.; Saeb, W.; Diem, S.; Herderich, M.; Schlauer, J. *Anal. Chem.* **2001**, *73*, 2571−2577.

(35) Bringmann, G.; God, R.; Schäffer, M. *Phytochemistry* **1996**, *43*, 1393−1403.

(36) (a) Bringmann, G.; Zagst, R.; Schöner, B.; Busse, H.; Hemmerling, M.; Burschka, C. *Acta Crystallogr., Sect. C: Cryst. Struct. Commun.* **1991**, *47*, 1703−1705. (b) Bringmann, G.; Rübenacker, M.;

DOI: 10.1021/acs.jnatprod.9b00755
J. Nat. Prod. 2019, 82, 3150−3164

Vogt, P.; Busse, H.; Akè Assi, L.; Peters, K.; von Schnering, H. G. *Phytochemistry* **1991**, *30*, 1691−1696. (c) Bringmann, G.; Ortmann, T.; Zagst, R.; Schöner, B.; Aké Assi, L.; Burschka, C. *Phytochemistry* **1992**, *31*, 4015−4018.
(37) (a) Ruangrungsi, N.; Wongpanich, Y.; Tantivatana, P.; Cowe, H. J.; Cox, P. J. *J. Nat. Prod.* **1985**, *48*, 529−535. (b) Parthasarathy, P. C.; Kartha, G. *Indian J. Chem.* **1983**, *22B*, 590−591. (c) Govindachari, T. R.; Nagarajan, K.; Parthasarathy, P. C.; Rajagopalan, T. G.; Desai, H. K.; Chen, S. M. L.; Nakanishi, K. *J. Chem. Soc., Perkin Trans. 1* **1974**, 1413−1417.
(38) For a significant exception, in which the chromophore connected to the stereogenic center chiroptically dominates the biaryl system, see: Bracher, F.; Eisenreich, W. J.; Mühlbacher, J.; Dreyer, M.; Bringmann, G. *J. Org. Chem.* **2004**, *69*, 8602−8608.
(39) Luková, K.; Nesvadba, R.; Uhliková, T.; Obenchain, D. A.; Wachsmuth, D.; Grabow, J.-U.; Urban, S. *Phys. Chem. Chem. Phys.* **2018**, *20*, 14664−14670.
(40) Neese, F. *Wiley Interdiscip. Rev. Comput. Mol. Sci.* **2012**, *2*, 73−78.
(41) (a) Ansari, D.; Tingstedt, B.; Andersson, B.; Holmquist, F.; Sturesson, C.; Williamson, C.; Sasor, A.; Borg, D.; Bauden, M.; Andersson, B. *Future Oncol.* **2016**, *12*, 1929−1946. (b) Hidalgo, M. *N. Engl. J. Med.* **2010**, *362*, 1605−1617.
(42) (a) Bardeesy, N.; DePinho, R. A. *Nat. Rev. Cancer* **2002**, *2*, 897−909. (b) Strimpakos, A.; Saif, M. W.; Syrigos, K. N. *Cancer Metastasis Rev.* **2008**, *27*, 495−522.
(43) (a) Nath, S.; Daneshvar, K.; Roy, L. D.; Grover, P.; Kidiyoor, A.; Mosley, L.; Sahraei, M.; Mukherjee, P. *Oncogenesis* **2013**, *2*, No. e51. (b) Long, J.; Zhang, Y.; Yu, X.; Yang, J.; LeBru, D. G.; Chen, C.; Yao, Q.; Li, M. *Expert Opin. Ther. Targets* **2011**, *15*, 817−828.
(44) (a) Garrido-Laguna, I.; Hidalgo, M. *Nat. Rev. Clin. Oncol.* **2015**, *12*, 319−334. (b) Teague, A.; Lim, K.-H.; Wang-Gillam, A. *Ther. Adv. Med. Oncol.* **2015**, *7*, 68−84.
(45) Izuishi, K.; Kato, K.; Ogura, T.; Kinoshita, T.; Esumi, H. *Cancer Res.* **2000**, *60*, 6201−6207.
(46) Awale, S.; Lu, J.; Kalauni, S. K.; Kurashima, Y.; Tezuka, Y.; Kadota, S.; Esumi, H. *Cancer Res.* **2006**, *66*, 1751−1757.
(47) Magolan, J.; Coster, M. J. *Curr. Drug Delivery* **2010**, *7*, 355−369.
(48) (a) Awale, S.; Ueda, J.; Athikomkulchai, S.; Abdelhamed, S.; Yokoyama, S.; Saiki, I.; Miyatake, R. *J. Nat. Prod.* **2012**, *75*, 1177−1183. (b) Ueda, J.; Athikomkulchai, S.; Miyatake, R.; Saiki, I.; Esumi, H.; Awale, S. *Drug Des., Dev. Ther.* **2013**, *8*, 39−47.
(49) (a) Nguyen, H. X.; Do, T. N. V.; Le, T. H.; Nguyen, M. T. T.; Nguyen, N. T.; Esumi, H.; Awale, S. *J. Nat. Prod.* **2016**, *79*, 2053−2059. (b) Nguyen, N. T.; Nguyen, M. T. T.; Nguyen, H. X.; Dang, P. H.; Dibwe, D. F.; Esumi, H.; Awale, S. *J. Nat. Prod.* **2017**, *80*, 141−148. (c) Nguyen, H. X.; Nguye, M. T. T.; Nguyen, N. T.; Awale, S. *J. Nat. Prod.* **2017**, *80*, 2345−2352. (d) Li, J.; Seupel, R.; Bruhn, T.; Feineis, D.; Kaiser, M.; Brun, R.; Mudogo, V.; Awale, S.; Bringmann, G. *J. Nat. Prod.* **2017**, *80*, 2807−2817.
(50) (a) Bruhn, T.; Schaumlöffel, A.; Hemberger, Y.; Bringmann, G. *Chirality* **2013**, *25*, 243−249. (b) Bruhn, T.; Schaumlöffel, A.; Hemberger, Y.; Pescitelli, G. *SpecDis*, Version 1.71; www.specdis-software.jimdo.com: Berlin, Germany, 2017.
(51) Sheldrick, G. M. *Acta Crystallogr., Sect. A: Found. Crystallogr.* **2008**, *64*, 112−122.
(52) Pescitelli, G.; Bruhn, T. *Chirality* **2016**, *28*, 466−474.
(53) (a) Grimme, S.; Ehrlich, S.; Goerigk, L. *J. Comput. Chem.* **2011**, *32*, 1456−1465. (b) Grimme, S.; Antony, J.; Ehrlich, S.; Krieg, H. *J. Chem. Phys.* **2010**, *132*, 154104−19.
(54) Izsak, R.; Neese, F. *J. Chem. Phys.* **2011**, *135*, 144105−11.
(55) Orhan, I.; Şener, B.; Kaiser, M.; Brun, R.; Tasdemir, D. *Mar. Drugs* **2010**, *8*, 47−58.
(56) Lu, J.; Kunimoto, S.; Yamazaki, Y.; Kaminishi, M.; Esumi, H. *Cancer Sci.* **2004**, *95*, 547−552.

DOI: 10.1021/acs.jnatprod.9b00755
J. Nat. Prod. 2019, 82, 3150−3164